WEAKLY SUPERVISED DISENTANGLEMENT WITH GUARANTEES

Anonymous authors
Paper under double-blind review

ABSTRACT

Learning *disentangled* representations that correspond to factors of variation in real-world data is critical to interpretable and human-controllable machine learning. Recently, concerns about the viability of learning disentangled representations in a purely unsupervised manner has spurred a shift toward the incorporation of weak supervision. However, there is currently no formalism that identifies when and how weak supervision will guarantee disentanglement. To address this issue, we provide a theoretical framework—including a calculus of disentanglement—to assist in analyzing the disentanglement guarantees (or lack thereof) conferred by weak supervision when coupled with learning algorithms based on distribution matching. We empirically verify the guarantees and limitations of several weak supervision methods (restricted labeling, match-pairing, and rank-pairing), demonstrating the predictive power and usefulness of our theoretical framework.

1 INTRODUCTION

Many real-world data can be intuitively described via a data-generating process that first samples an underlying set of interpretable factors, and then—conditional on those factors—generate an observed data point. For example, in image generation, one might first generate the object identity and pose, and then build an image of this object accordingly. The goal of disentangled representation learning is to learn a distributed representation where each representation axis measures a distinct *factor of variation* in the dataset (Bengio et al., 2013). Learning such representations that align with the underlying factors of variation is critical to the development of machine learning models that are explainable or human-controllable (Gilpin et al., 2018; Lee et al., 2019; Klys et al., 2018).

In recent years, disentanglement research has focused on the learning of such representations in an *unsupervised* fashion, using only independent samples from the data distribution without access to the true factors of variation (Higgins et al., 2017; Chen et al., 2018a; Kim & Mnih, 2018; Esmaeili et al., 2018). However, Locatello et al. (2019) demonstrated that many existing methods for the unsupervised learning of disentangled representations are brittle, requiring careful supervision-based hyperparameter tuning. To build robust disentangled representation learning methods that do not require large amounts of supervised data, recent work has turned to forms of weak supervision (Chen & Batmanghelich, 2019; Gabbay & Hoshen, 2019). Weak supervision can allow one to build models that have interpretable representations even when human labeling is challenging, for example hair style in face generation, or style in music generation. While existing methods based on weakly-supervised learning demonstrate empirical gains, there is no formalism for describing the theoretical guarantees conferred by different forms of weak supervision that has been presented in prior work (Kulkarni et al., 2015; Reed et al., 2015; Bouchacourt et al., 2018).

In this paper, we present a comprehensive theoretical framework for weakly supervised disentanglement, and evaluate our framework on several datasets. Our contributions are several-fold.

1. We formalize weakly-supervised learning as distribution matching in an extended space.
2. We propose a set of definitions for disentanglement that can handle correlated factors and are inspired by many existing definitions in the literature (Higgins et al., 2018; Suter et al., 2018; Ridgeway & Mozer, 2018).
3. Using these definitions, we provide a conceptually useful and theoretically rigorous calculus of disentanglement.

4. We apply our theoretical framework of disentanglement to analyze the theoretical guarantees of three notable weak supervision methods (restricted labeling, match pairing, and rank pairing) and experimentally verify these guarantees.

2 FROM UNSUPERVISED TO WEAKLY SUPERVISED DISTRIBUTION MATCHING

Our goal in disentangled representation learning is to identify a latent-variable generative model whose latent variables correspond to ground truth factors of variation in the data. To identify the role that weak supervision plays in providing guarantees on disentanglement, we first formalize the model families we are considering, the forms of weak supervision, and finally the metrics we will use to evaluate and prove components of disentanglement.

We consider data-generating processes where $S \in \mathbb{R}^n$ are the factors of variation, with distribution $p^*(s)$, and $X \in \mathbb{R}^m$ is the observed data point which is a deterministic function of S, i.e., $X = g^*(S)$. Many existing algorithms in *unsupervised* learning of disentangled representations aim to learn a latent-variable model with prior $p(z)$ and generator g, where $g(Z) \overset{d}{=} g^*(S)$. However, simply matching the marginal distribution over data is not enough: the learned latent variables Z and the true generating factors S could still be entangled with each other (Locatello et al., 2019).

To address the failures of unsupervised learning of disentangled representations, we leverage weak supervision, where information about the data-generating process is conveyed through additional observations. By performing distribution matching on an augmented space (instead of just on the observation of X), we can provide guarantees on learned representations.

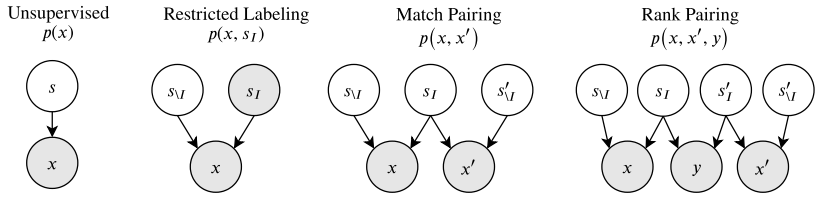

Figure 1: Augmented data distributions derived from weak supervision. Shaded nodes denote observed quantities, and unshaded nodes represent unobserved (latent) variables.

We consider three practical forms of weak supervision: restricted labeling, match pairing, and rank pairing. All of these forms of supervision can be thought of as augmented forms of the original joint distribution, where we partition the latent variables in two $S = (S_I, S_{\setminus I})$, and either observe a subset of the latent variables or share latents between multiple samples. A visualization of these augmented distributions is presented in Figure 1, and below we detail each form of weak supervision.

In **restricted labeling**, we observe a subset of the ground truth factors, S_I in addition to X. This allows us to perform distribution matching on $p^*(s_I, x)$, the joint distribution over data and observed factors, instead of just the data, $p^*(x)$, as in unsupervised learning. This form of supervision is often leveraged in style-content disentanglement, where labels are available for content but not style (Kingma et al., 2014; Narayanaswamy et al., 2017; Chen et al., 2018b; Gabbay & Hoshen, 2019).

Match Pairing uses paired data, (x, x') that share values for a known subset of factors, s_I. This is a weaker form of supervision than restricted labeling, as the learning algorithm no longer depends on the underlying value s_I. Several variants of match pairing have appeared in the literature (Kulkarni et al., 2015; Bouchacourt et al., 2018; Ridgeway & Mozer, 2018), but typically focus on groups of observations in contrast to the paired setting we consider here.

Rank Pairing is another form of paired data generation where the pairs (x, x') are generated in an i.i.d. fashion, and an additional indicator variable y is observed that determines whether the corresponding latent s_i is greater than s'_i: $y = \mathbf{1}\{s_i \geq s'_i\}$. Although supervision via ranking features prominently in the metric learning literature (McFee & Lanckriet, 2010; Wang et al., 2014), our focus in this paper will be on rank pairing in the context of disentanglement guarantees.

For each form of weak supervision, we can train generative models with the same structure as in Figure 1, using data sampled from the ground truth model and a distribution matching objective. For example, for match pairing, we train a generative model $(p(z), g)$ such that the paired random variable $(g(Z_I, Z_{\setminus I}), g(Z_I, Z'_{\setminus I}))$ from the generator matches the distribution of the corresponding paired random variable $(g^*(S_I, S_{\setminus I}), g^*(S_I, S'_{\setminus I}))$ from the augmented data distribution.

3 Defining Disentanglement

To identify the role that weak supervision plays in providing guarantees on disentanglement, we introduce a set of definitions that are consistent with our intuitions about what constitutes "disentanglement" and amenable to theoretical analysis. Our new definitions decompose disentanglement into two distinct concepts: consistency and restrictiveness. Different forms of weak supervision can enable consistency or restrictiveness on subsets of factors, and in Section 4 we build up a calculus of disentanglement from these primitives. We discuss the relationship to prior definitions of disentanglement in Appendix A.

3.1 Decomposing Disentanglement into Consistency and Restrictiveness

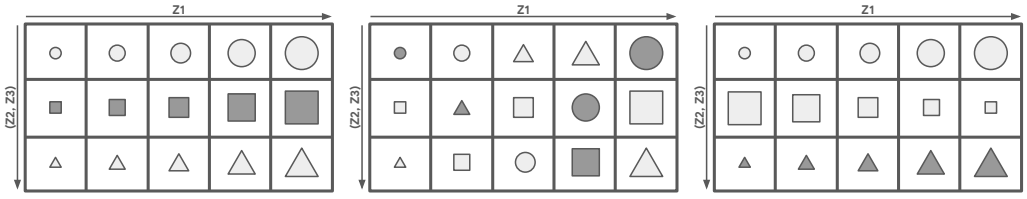

(a) Disentanglement (b) Consistency (c) Restrictiveness

Figure 2: Illustration of disentanglement, consistency, and restrictiveness of z_1 with respect to the factor of variation *size*. Each image of a shape represents the decoding $g(z_{1:3})$ by the generative model. Each column denotes a fixed choice of z_1. Each row denotes a fixed choice of (z_2, z_3). For simplicity of illustration, we omit the consideration of nuisance variables.

To ground our discussion of disentanglement in a concrete example, we shall consider an oracle that generates shapes, with the underlying factors of variation *size* (S_1), *shape* (S_2), and *color* (S_3). We now wish to determine whether Z_1 of our generative model disentangles the concept of size. Intuitively, one way to check whether Z_1 of the generative model disentangles *size* (S_1) is to visually inspect what happens as we vary Z_1, Z_2, and Z_3, and see whether the resulting visualizations are consistent with Figure 2a. In doing so, our visual inspection checks for two properties:

1. When Z_1 is fixed, the *size* (S_1) of the generated object never changes.
2. When Z_1 is changed, the change is restricted to the *size* (S_1) of the generated object.

We thus argue that disentanglement decomposes into these two properties, which we refer to as *generator consistency* and *generator restrictiveness*. We shall formalize these two properties.

Let $\mathcal{H}$ be a hypothesis class of generative models from which we assume the true data-generating function is drawn. Each element of the hypothesis class $\mathcal{H}$ is a tuple $(p(s), g, e)$, where $p(s)$ describes the distribution over factors of variation, the generator g is a function that maps from the factor space $\mathcal{S} \in \mathbb{R}^n$ to the observation space $\mathcal{X} \in \mathbb{R}^m$, and the encoder e is a function that maps from $\mathcal{X} \to \mathcal{S}$. S and X can consist of both discrete and continuous random variables. We impose a few mild assumptions on $\mathcal{H}$ (see Appendix H.1). Notably, we assume every factor of variation is exactly recoverable from the observation X, i.e. $e(g(S)) = S$.

Given an oracle model $h^* = (p^*, g^*, e^*) \in \mathcal{H}$, we would like to learn a model $h = (p, g, e) \in \mathcal{H}$ whose latent variables disentangle the latent variables in h^*. We refer to the latent-variables in the oracle h^* as S and the alternative model h's latent variables as Z. If we further restrict h to only those models where $g(Z) \overset{d}{=} g^*(S)$ are equal in distribution, it is natural to align Z and S via

$S = e^* \circ g(Z)$. Under this relation between Z and S, our goal is to construct definitions that describe whether the latent code Z_i disentangles the corresponding factor S_i.

Generator Consistency. Let I denote a set of indices and p_I denote the generating process

$$z_I \sim p(z_I) \tag{1}$$

$$z_{\setminus I}, z'_{\setminus I} \overset{\text{iid}}{\sim} p(z_{\setminus I} \mid z_I). \tag{2}$$

This generating process samples Z_I once and then conditionally samples Z_I twice in an i.i.d. fashion. We say that Z_I is consistent with S_I if

$$\mathbb{E}_{p_I} \| e^*_I \circ g(z_I, z_{\setminus I}) - e^*_I \circ g(z_I, z'_{\setminus I}) \|^2 = 0, \tag{3}$$

where e^*_I is the oracle encoder restricted to the indices I.

Intuitively, Equation (3) states that, for any fixed choice of Z_I, resampling of $Z_{\setminus I}$ will not influence the oracle's measurement of the factors S_I. Here, our assumption that $g(Z)$ is identical in distribution to $g^*(S)$ ensures that samples from the generative model remain within the domain of definition of the oracle encoder e^*. An illustration of a generative model where Z_1 is consistent with *size* (S_1) is provided in Figure 2b.

Generator Restrictiveness. Let $p_{\setminus I}$ denote the generating process

$$z_{\setminus I} \sim p(z_{\setminus I}) \tag{4}$$

$$z_I, z'_I \overset{\text{iid}}{\sim} p(z_I \mid z_{\setminus I}). \tag{5}$$

We say that Z_I is restricted to S_I if

$$\mathbb{E}_{p_{\setminus I}} \| e^*_{\setminus I} \circ g(z_I, z_{\setminus I}) - e^*_{\setminus I} \circ g(z'_I, z_{\setminus I}) \|^2 = 0. \tag{6}$$

Equation (6) states that, for any fixed choice of $Z_{\setminus I}$, resampling of Z_I will not influence the oracle's measurement of the factors $S_{\setminus I}$. Thus, changing Z_I is restricted to modifying only S_I. An illustration of a generative model where Z_1 is restricted to *size* (S_1) is provided in Figure 2c.

Generator Disentanglement. We now say that Z_I disentangles S_I if Z_I is consistent with *and* restricted to S_I. If we denote consistency and restrictiveness via Boolean functions $C(I)$ and $R(I)$, we can now concisely state that

$$D(I) := C(I) \wedge R(I), \tag{7}$$

where $D(I)$ denotes whether Z_I disentangles S_I. An illustration of a generative model where Z_1 disentangles *size* (S_1) is provided in Figure 2a. Note that while size increases monotonically with Z_1 in the figure for convenience of illustration, we wish to clarify that monotonicity is orthogonal to the concepts of consistency and restrictiveness.

3.2 Encoder-Based Definitions for Disentanglement

Our proposed definitions are asymmetric—measuring the behavior of a generative model against an encoder. So far, we have chosen to present the definitions from the perspective of a learned generator (p, g) measured against an oracle encoder e^*. In this sense, they are *generator-based* definitions. We can also develop a parallel set of definitions for *encoder-based* consistency, restrictiveness, and disentanglement within our framework simply by using an oracle generator (p^*, g^*) measured against a learned encoder e. We only present consistency for brevity.

Encoder Consistency. Let p^*_I denote the generating process

$$s_I \sim p^*(s_I) \tag{8}$$

$$s_{\setminus I}, s'_{\setminus I} \overset{\text{iid}}{\sim} p^*(s_{\setminus I}, \mid s_I). \tag{9}$$

We say that S_I is consistent with Z_I if

$$\mathbb{E}_{p^*_I} \| e_I \circ g^*(s_I, s_{\setminus I}) - e_I \circ g^*(s_I, s'_{\setminus I}) \|^2 = 0. \tag{10}$$

We now make two important observations. First, a valuable trait of our encoder-based definitions is that one can check for encoder consistency / restrictiveness / disentanglement *as long as one*

has access to match pairing data from the oracle generator. This is in contrast to the existing disentanglement definitions and metrics, which require access to the ground truth factors (Higgins et al., 2017; Kim & Mnih, 2018; Chen et al., 2018a; Suter et al., 2018; Ridgeway & Mozer, 2018; Eastwood & Williams, 2018). The ability to check for our definitions in a weakly supervised fashion is the key to why we can develop a theoretical framework using the language of consistency and restrictiveness. Second, encoder-based definitions are tractable to measure when testing on synthetic data, since the synthetic data directly serves the role of the oracle generator. As such, while we develop our theory to guarantee *both* generator-based and the encoder-based disentanglement, all of our measurements in the experiments will be conducted with respect to a learned encoder.

We make two remarks on notations. First, $D(i) := D(\{i\})$. Second, $D(\varnothing)$ evaluates to true. We apply these conventions to C and R analogously. Finally, $D(I), C(I), R(I)$ are implicitly dependent on either (p, g, e^*) (generator-based) or (p^*, g^*, e) (encoder-based). Where important, we shall make this dependency explicit (e.g., let $D(I\,; p, g, e^*)$ denote generator-based disentanglement).

4 A Calculus of Disentanglement

We note several interesting relationships between restrictiveness and consistency. First, by definition, $C(I)$ is equivalent to $R(\backslash I)$. Second, we can see from Figures 2b and 2c that $C(I)$ and $R(I)$ do not imply each other. Based on these observations and given that consistency and restrictiveness operate over *subsets* of the random variables, a natural question that arises is whether consistency or restrictiveness over certain sets of variables imply additional properties over other sets of variables. We develop a calculus for discovering *implied* relationships between learned latent variables Z and ground truth factors of variation S given known relationships as follows.

Calculus of Disentanglement

Consistency and Restrictiveness

$$C(I) \not\Longrightarrow R(I) \qquad R(I) \not\Longrightarrow C(I) \qquad C(I) \iff R(\backslash I)$$

Union Rules

$$C(I) \wedge C(J) \implies C(I \cup J) \qquad R(I) \wedge R(J) \implies R(I \cup J)$$

Intersection Rules

$$C(I) \wedge C(J) \implies C(I \cap J) \qquad R(I) \wedge R(J) \implies R(I \cap J)$$

Full Disentanglement

$$\textstyle\bigwedge_{i=1}^{n} C(i) \iff \bigwedge_{i=1}^{n} D(i) \qquad \bigwedge_{i=1}^{n} R(i) \iff \bigwedge_{i=1}^{n} D(i)$$

Our calculus provides a theoretically rigorous procedure for reasoning about disentanglement. In particular, it is no longer necessary to prove whether the supervision method of interest satisfies consistency and restrictiveness for each and every factor. Instead, it suffices to show that a supervision method guarantees consistency or restrictiveness for a subset of factors, and then combine multiple supervision methods via the calculus to guarantee full disentanglement. We can also use the calculus to gain consistency of individual factors when weak supervision is available only for sets of variables. For example, achieving consistency on $S_{1,2}$ and $S_{2,3}$ implies consistency on S_2. Furthermore, these rules are also agnostic to using generator or encoder-based definitions. We defer the complete proofs to Appendix H.2.

5 Formalizing Weak Supervision with Guarantees

In this section, we address the important question of how to distinguish when disentanglement arises from the supervision method and when it comes from model inductive bias. This challenge was first put forth by Locatello et al. (2019), which noted that unsupervised disentanglement is heavily reliant on model inductive bias. As we transition toward supervised approaches, it is crucial that we formalize what it means for disentanglement to be guaranteed by weak supervision.

Sufficiency for Disentanglement. Let $\mathcal{P}$ denote a family of augmented distributions. We say that a weak supervision method $\mathbf{S} : \mathcal{H} \to \mathcal{P}$ is *sufficient* for learning a generator whose latent codes Z_I disentangle the factors S_I if there exists a learning algorithm $\mathcal{A} : \mathcal{P} \to \mathcal{H}$ such that for any choice of

$(p^*(s), g^*, e^*) \in \mathcal{H}$, the procedure $\mathcal{A} \circ \mathbf{S}(p^*(s), g^*, e^*)$ returns a model $(p(z), g, e)$ for which both $D(I\,; p, g, e^*)$ and $D(I\,; p^*, g^*, e)$ hold, and $g(Z) \overset{d}{=} g^*(S)$.

The key insight of this definition is that we force the strategy and learning algorithm pair $(\mathbf{S}, \mathcal{A})$ to handle all possible oracles drawn from the hypothesis class $\mathcal{H}$. This prevents the exploitation of model inductive bias, since any bias from the learning algorithm $\mathcal{A}$ toward a reduced hypothesis class $\hat{\mathcal{H}} \subset \mathcal{H}$ will result in failure to handle oracles in the complementary hypothesis class $\mathcal{H} \setminus \hat{\mathcal{H}}$.

The distribution matching requirement $g(Z) \overset{d}{=} g^*(S)$ ensures latent code informativeness, i.e., preventing trivial solutions where the latent code is uninformative (see Theorem 7 for formal statement). Intuitively, distribution matching paired with a deterministic generator guarantees invertibility of the learned generator and encoder, enforcing that Z_I cannot encode less information than S_I (e.g., only encoding age group instead of numerical age) and vice versa.

6 Analysis of Weak Supervision Methods

We now apply our theoretical framework to three practical weak supervision methods: restricted labeling, match pairing, and rank pairing. Our main theoretical findings are that: (1) These methods can be applied in a targeted manner to provide single factor consistency or restrictiveness guarantees. (2) By enforcing consistency (or restrictiveness) on all factors, we can learn models with strong disentanglement performance. Correspondingly, Figure 3 and Figure 5 are our main experimental results, demonstrating that these theoretical guarantees have predictive power in practice.

6.1 Theoretical Guarantees from Weak Supervision

We prove that if a training algorithm successfully matches the generated distribution to data distribution generated via restricted labeling, match pairing, or rank pairing of factors S_I, then Z_I is guaranteed to be *consistent* with S_I:

Theorem 1. *Given any oracle $(p^*(s), g^*, e^*) \in \mathcal{H}$, consider the distribution-matching algorithm $\mathcal{A}$ that selects a model $(p(z), g, e) \in \mathcal{H}$ such that:*

1. $(g^*(S), S_I) \overset{d}{=} (g(Z), Z_I)$ ***(Restricted Labeling)**; or*
2. $\left(g^*(S_I, S_{\setminus I}), g^*(S_I, S'_{\setminus I})\right) \overset{d}{=} \left(g(Z_I, Z_{\setminus I}), g(Z_I, Z'_{\setminus I})\right)$ ***(Match Pairing)**; or*
3. $(g^*(S), g^*(S'), \mathbf{1}\{S_i \leq S'_i\}) \overset{d}{=} (g(Z), g(Z'), \mathbf{1}\{Z_i \leq Z'_i\})$ **(Rank Pairing)**.

Then (p, g) satisfies $C(I\,; p, g, e^*)$ and e satisfies $C(I\,; p^*, g^*, e)$.

Note that the same supervision does not guarantee that Z_I is restricted to S_I (Theorem 9). Fortunately, we can see from the calculus that if we also have restricted labeling for $S_{\setminus I}$, or match pairing for $S_{\setminus I}$, then we have guaranteed $R(I) \wedge C(I)$ implying disentanglement of factor I. In the experiments below, we empirically verify the theoretical guarantees provided in Theorem 1.

6.2 Experiments

We conducted experiments on five prominent datasets in the disentanglement literature: *Shapes3D* (Kim & Mnih, 2018), *dSprites* (Higgins et al., 2017), *Scream-dSprites* (Locatello et al., 2019), *SmallNORB* (LeCun et al., 2004), and *Cars3D* (Reed et al., 2015). Since some of the underlying factors are treated as nuisance variables in SmallNORB and Scream-dSprites, we show in Appendix B that our theoretical framework can be easily adapted accordingly to handle such situations. We use generative adversarial networks (GANs, Goodfellow et al. (2014)) for learning (p, g) but any distribution matching algorithm (e.g. maximum likelihood training in tractable models, or VI in latent-variable models) could be applied. Our results are collected over a broad range of hyperparameter configurations (see Appendix G for details).

Since existing quantitative metrics of disentanglement all measure the performance of an encoder with respect to the true data generator, we trained an encoder *post-hoc* to approximately invert

the learned generator, and measured all quantitative metrics (e.g. mutual information gap) on the encoder. Our theory assumes that the learned generator must be invertible. While this is not true for conventional GANs, our empirical results show that this is not an issue in practice (see Appendix F).

We present three sets of experimental results: (1) Single-factor experiments, where we show that our theory can be applied in a *targeted* fashion to guarantee consistency or restrictiveness of a single factor. (2) Consistency versus restrictiveness experiments, where we show the extent to which single-factor consistency and restrictiveness are correlated even when the models are only trained to maximize one or the other. (3) Full disentanglement experiments, where we apply our theory to fully disentangle all factors. A more extensive set of experiments can be found in the Appendix.

6.2.1 Single-Factor Consistency and Restrictiveness

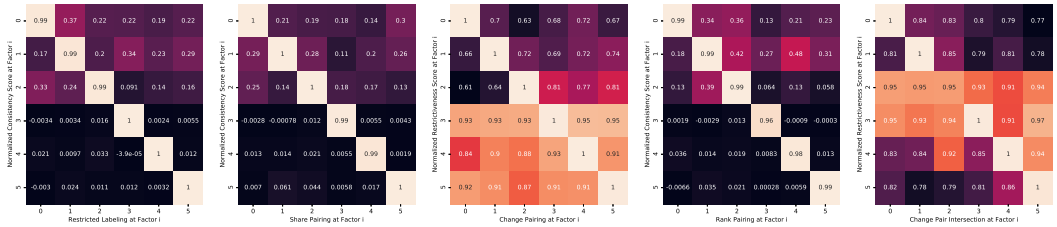

Figure 3: Heatmap visualization of ablation studies that measure either single-factor consistency or single-factor restrictiveness as a function of various supervision methods, conducted on Shapes3D. Our theory predicts the diagonal components to achieve the highest scores. Note that share pairing, change pairing, and change pair intersection are special cases of match pairing.

We empirically verify that single-factor consistency or restrictiveness can be achieved with the supervision methods of interest. Note there are two special cases of match pairing: one where S_i is the only factor that is shared between x and x' and one where S_i is the only factor that is changed. We distinguish these two conditions as *share pairing* and *change pairing*, respectively. Theorem 1 shows that restricted labeling, share pairing, and rank pairing of the i^{th} factor are each sufficient supervision strategies for guaranteeing consistency on S_i. Change pairing at S_i is equivalent to share pairing at $S_{\setminus i}$; the complement rule $C(I) \iff R(\setminus I)$ allows us to conclude that change pairing guarantees restrictiveness. The first four heatmaps in Figure 3 show the results for restricted labeling, share pairing, change pairing, and rank pairing. The numbers shown in the heatmap are the *normalized consistency and restrictiveness scores*. We define the normalized consistency score as

$$\tilde{c}(I\,; p^*, g^*, e) = 1 - \frac{\mathbb{E}_{p_I^*} \|e_I \circ g^*(s_I, s_{\setminus I}) - e_I \circ g^*(s_I, s'_{\setminus I})\|^2}{\mathbb{E}_{s, s' \overset{\text{iid}}{\sim} p^*} \|e_I \circ g^*(s) - e_I \circ g^*(s')\|^2}. \tag{11}$$

This score is bounded on the interval $[0, 1]$ and is maximal when $C(I; p^*, g^*, e)$ is satisfied. This normalization procedure is similar in spirit to that used in Suter et al. (2018)'s Interventional Robustness Score. The normalized restrictiveness score $\tilde{r}$ can be analogously defined.

The final heatmap in Figure 3 demonstrates the calculus of intersection. In practice, it may be easier to acquire paired data where multiple factors change simultaneously. If we have access to two kinds of datasets, one where S_I are changed and one where S_J are changed, our calculus predicts that training on both datasets will guarantee restrictiveness on $S_{I \cap J}$. The final heatmap shows six such intersection settings and measures the normalized restrictiveness score; in all but one setting, the results are consistent with our theory. We show in Figure 6 that this inconsistency is attributable to the failure of the GAN to distribution-match due to sensitivity to a specific hyperparameter.

6.2.2 Consistency versus Restrictiveness

We now determine the extent to which consistency and restrictiveness are correlated in practice. In Figure 4, we collected all 864 Shapes3D models that we trained in Section 6.2.1 and measured the consistency and restrictiveness of each model on each factor, providing both the correlation plot and scatterplots of $\tilde{c}(i)$ versus $\tilde{r}(i)$. Since the models trained in Section 6.2.1 only ever targeted the consistency *or* restrictiveness of a single factor, and since our calculus demonstrates that consistency

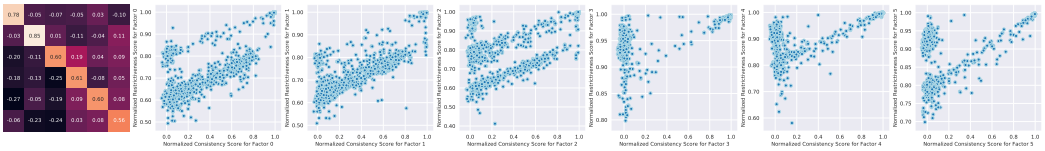

Figure 4: Correlation plot and scatterplots demonstrating the empirical relationship between $\tilde{c}(i)$ and $\tilde{r}(i)$ across all 864 models trained on Shapes3D.

and restrictiveness do not imply each other, one might *a priori* expect to find no correlation in Figure 4. Our results show that the correlation is actually quite strong. Since this correlation is not guaranteed by our choice of weak supervision, it is necessarily a consequence of model inductive bias. We believe this correlation between consistency and restrictiveness to have been a general source of confusion in the disentanglement literature, causing many to either observe or believe that restricted labeling or share pairing on S_i (which only guarantees consistency) is sufficient for disentangling S_i (Kingma et al., 2014; Chen & Batmanghelich, 2019; Gabbay & Hoshen, 2019; Narayanaswamy et al., 2017). It remains an open question why consistency and restrictiveness are so strongly correlated when training existing models on real-world data.

6.2.3 Full Disentanglement

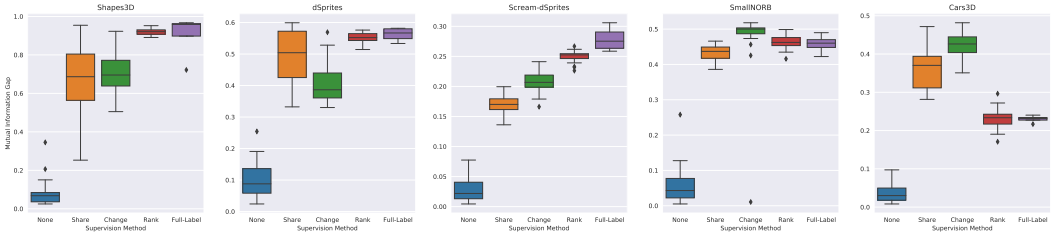

Figure 5: Disentanglement performance of a vanilla GAN, share pairing GAN, change pairing GAN, rank pairing GAN, and fully-labeled GAN, as measured by the mutual information gap across several datasets. A comprehensive set of performance evaluations on existing disentanglement metrics is available in Figure 12.

If we have access to share / change / rank-pairing data for each factor, our calculus states that it is possible to guarantee full disentanglement. We trained our generative model on either complete share pairing, complete change pairing, or complete rank pairing, and measured disentanglement performance via the discretized mutual information gap (Chen et al., 2018a; Locatello et al., 2019). As negative and positive controls, we also show the performance of an unsupervised GAN and a fully-supervised GAN where the latents are fixed to the ground truth factors of variation. Our results in Figure 5 empirically verify that combining single-factor weak supervision datasets leads to consistently high disentanglement scores.

7 Conclusion

In this work, we construct a theoretical framework to rigorously analyze the disentanglement guarantees of weak supervision algorithms. Our paper clarifies several important concepts, such as consistency and restrictiveness, that have been hitherto confused or overlooked in the existing literature, and provides a formalism that precisely distinguishes when disentanglement arises from supervision versus model inductive bias. Through our theory and a comprehensive set of experiments, we demonstrated the conditions under which various supervision strategies *guarantee* disentanglement. Our work establishes several promising directions for future research. First, we hope that our formalism and experiments inspire greater theoretical and scientific scrutiny of the inductive biases present in existing models. Second, we encourage the search for other learning algorithms (besides distribution-matching) that may have theoretical guarantees when paired with the right form of supervision. Finally, we hope that our framework enables the theoretical analysis of other promising weak supervision methods.

REFERENCES

Yoshua Bengio, Aaron Courville, and Pascal Vincent. Representation learning: A review and new perspectives. *IEEE transactions on pattern analysis and machine intelligence*, 35(8):1798–1828, 2013.

Diane Bouchacourt, Ryota Tomioka, and Sebastian Nowozin. Multi-level variational autoencoder: Learning disentangled representations from grouped observations. In *Thirty-Second AAAI Conference on Artificial Intelligence*, 2018.

Junxiang Chen and Kayhan Batmanghelich. Weakly supervised disentanglement by pairwise similarities. *arXiv preprint arXiv:1906.01044*, 2019.

Tian Qi Chen, Xuechen Li, Roger B Grosse, and David K Duvenaud. Isolating sources of disentanglement in variational autoencoders. *Advances in Neural Information Processing Systems*, pp. 2610–2620, 2018a.

Yutian Chen, Yannis Assael, Brendan Shillingford, David Budden, Scott Reed, Heiga Zen, Quan Wang, Luis C Cobo, Andrew Trask, Ben Laurie, et al. Sample efficient adaptive text-to-speech. *arXiv preprint arXiv:1809.10460*, 2018b.

Cian Eastwood and Christopher KI Williams. A framework for the quantitative evaluation of disentangled representations. *ICLR*, 2018.

Babak Esmaeili, Hao Wu, Sarthak Jain, Alican Bozkurt, Narayanaswamy Siddharth, Brooks Paige, Dana H Brooks, Jennifer Dy, and Jan-Willem van de Meent. Structured disentangled representations. *arXiv preprint arXiv:1804.02086*, 2018.

Aviv Gabbay and Yedid Hoshen. Latent optimization for non-adversarial representation disentanglement. *arXiv preprint arXiv:1906.11796*, 2019.

Leilani H Gilpin, David Bau, Ben Z Yuan, Ayesha Bajwa, Michael Specter, and Lalana Kagal. Explaining explanations: An overview of interpretability of machine learning. In *2018 IEEE 5th International Conference on data science and advanced analytics (DSAA)*, pp. 80–89. IEEE, 2018.

Ian Goodfellow, Jean Pouget-Abadie, Mehdi Mirza, Bing Xu, David Warde-Farley, Sherjil Ozair, Aaron Courville, and Yoshua Bengio. Generative adversarial nets. In *Advances in neural information processing systems*, pp. 2672–2680, 2014.

Irina Higgins, Loic Matthey, Arka Pal, Christopher Burgess, Xavier Glorot, Matthew Botvinick, Shakir Mohamed, and Alexander Lerchner. beta-vae: Learning basic visual concepts with a constrained variational framework. *ICLR*, 2(5):6, 2017.

Irina Higgins, David Amos, David Pfau, Sebastien Racaniere, Loic Matthey, Danilo Rezende, and Alexander Lerchner. Towards a definition of disentangled representations. *arXiv preprint arXiv:1812.02230*, 2018.

Hyunjik Kim and Andriy Mnih. Disentangling by factorising. *ICML*, 2018.

Durk P Kingma, Shakir Mohamed, Danilo Jimenez Rezende, and Max Welling. Semi-supervised learning with deep generative models. *Advances in neural information processing systems*, pp. 3581–3589, 2014.

Jack Klys, Jake Snell, and Richard Zemel. Learning latent subspaces in variational autoencoders. In *Advances in Neural Information Processing Systems*, pp. 6444–6454, 2018.

Tejas D Kulkarni, William F Whitney, Pushmeet Kohli, and Josh Tenenbaum. Deep convolutional inverse graphics network. In *Advances in neural information processing systems*, pp. 2539–2547, 2015.

Yann LeCun, Fu Jie Huang, Leon Bottou, et al. Learning methods for generic object recognition with invariance to pose and lighting. In *CVPR (2)*, pp. 97–104. Citeseer, 2004.

Hsin-Ying Lee, Hung-Yu Tseng, Qi Mao, Jia-Bin Huang, Yu-Ding Lu, Maneesh Singh, and Ming-Hsuan Yang. Drit++: Diverse image-to-image translation via disentangled representations. *arXiv preprint arXiv:1905.01270*, 2019.

Francesco Locatello, Stefan Bauer, Mario Lucic, Sylvain Gelly, Bernhard Schölkopf, and Olivier Bachem. Challenging common assumptions in the unsupervised learning of disentangled representations. *ICML*, 2019.

Brian McFee and Gert R Lanckriet. Metric learning to rank. In *Proceedings of the 27th International Conference on Machine Learning (ICML-10)*, pp. 775–782, 2010.

Takeru Miyato and Masanori Koyama. cgans with projection discriminator. *arXiv preprint arXiv:1802.05637*, 2018.

Siddharth Narayanaswamy, T Brooks Paige, Jan-Willem Van de Meent, Alban Desmaison, Noah Goodman, Pushmeet Kohli, Frank Wood, and Philip Torr. Learning disentangled representations with semi-supervised deep generative models. In *Advances in Neural Information Processing Systems*, pp. 5925–5935, 2017.

Scott E Reed, Yi Zhang, Yuting Zhang, and Honglak Lee. Deep visual analogy-making. In *Advances in neural information processing systems*, pp. 1252–1260, 2015.

Karl Ridgeway and Michael C Mozer. Learning deep disentangled embeddings with the f-statistic loss. *Advances in Neural Information Processing Systems*, pp. 185–194, 2018.

Raphael Suter, Dorde Miladinovic, Stefan Bauer, and Bernhard Schölkopf. Interventional robustness of deep latent variable models. *ICML*, 2018.

Jiang Wang, Yang Song, Thomas Leung, Chuck Rosenberg, Jingbin Wang, James Philbin, Bo Chen, and Ying Wu. Learning fine-grained image similarity with deep ranking. In *Proceedings of the IEEE Conference on Computer Vision and Pattern Recognition*, pp. 1386–1393, 2014.

Our appendix consists of eight sections. We provide a brief summary of each section below.

Appendix A: We elaborate on the connections between existing definitions of disentanglement and our definitions of consistency / restrictiveness / disentanglement. In particular, we highlight three notable properties of our definitions not present in many existing definitions.

Appendix B: We adapt our definitions to be able to handle nuisance variables. We do so through a simple modification of the definition of restrictiveness.

Appendix C: We show several additional single-factor experiments. We first address one of the results in the main text that is not consistent with our theory, and explain why it can be attributed to hyperparameter sensitivity. We next unwrap the heatmaps into more informative boxplots.

Appendix D: We provide an additional suite of consistency versus restrictiveness experiments by comparing the effects of training with share pairing (which guarantees consistency), change pairing (which guarantees restrictiveness), and *both*.

Appendix E: We provide full disentanglement results on all five datasets as measured according to six different metrics of disentanglement found in the literature.

Appendix F: We show visualizations of a weakly supervised generative model trained to achieve full disentanglement.

Appendix G: We describe the set of hyperparameter configurations used in all our experiments.

Appendix H: We provide the complete set of assumptions and proofs for our theoretical framework.

A Connections to Existing Definitions

Numerous definitions of disentanglement are present in the literature (Higgins et al., 2017; 2018; Kim & Mnih, 2018; Suter et al., 2018; Ridgeway & Mozer, 2018; Eastwood & Williams, 2018; Chen et al., 2018a). We mostly defer to the terminology suggested by Ridgeway & Mozer (2018), which decomposes disentanglement into *modularity*, *compactness*, and *explicitness*. Modularity means a latent code Z_i is predictive of at most one factor of variation S_j. Compactness means a factor of variation S_i is predicted by at most one latent code Z_j. And explicitness means a factor of variation S_j is predicted by the latent codes via a simple transformation (e.g. linear). Similar to Eastwood & Williams (2018); Higgins et al. (2018), we suggest a further decomposition of Ridgeway & Mozer (2018)'s explicitness into *latent code informativeness* and *latent code simplicity*. In this paper, we omit latent code simplicity from consideration. Since informativeness of the latent code is already enforced by our requirement that $g(Z)$ is equal in distribution to $g^*(S)$ (see Theorem 7), we focus on comparing our proposed concepts of consistency and restrictiveness to modularity and compactness. We make note of three important distinctions.

Restrictiveness is not synonymous with either modularity or compactness. In Figure 2c, it is evident the factor of variation *size* is not predictable any individual Z_i (conversely, Z_1 is not predictable from any individual factor S_i). As such, Z_1 is neither a modular nor compact representation of *size*, despite being restricted to *size*. To our knowledge, no existing quantitative definition of disentanglement (or its decomposition) specifically measures restrictiveness.

Consistency and restrictiveness are invariant to correlated factors of variation. Many existing definitions of disentanglement are instantiated by measuring the mutual information between Z and S. For example, Ridgeway & Mozer (2018) defines that a latent code Z_i to be "ideally modular" if it has high mutual information with a single factor S_j and zero mutual information with all other factors $S_{\setminus j}$. This presents a issue when the true factors of variation themselves are correlated; even if $Z_1 = S_1$, the latent code Z_1 would violate modularity if S_1 itself has positive mutual information with S_2. Consistency and restrictiveness circumvent this issue by relying on conditional resampling. Consistency, for example, only measures the extent to which S_I is *invariant* to resampling of $Z_{\setminus I}$ when conditioned on Z_I and is thus achieved as long as s_I is a function of only z_I—irrespective of whether s_I and $s_{\setminus I}$ are correlated. In this regard, our definitions draw inspiration from Suter et al. (2018)'s intervention-based definition but replaces the need for counterfactual reasoning with the simpler conditional sampling.

Consistency and restrictiveness arise in weak supervision guarantees. One of our goals is to propose definitions that are amenable to theoretical analysis. As we can see in Section 4, consistency and restrictiveness serve as the core primitive concepts that we use to describe disentanglement guarantees conferred by various forms of weak supervision.

B HANDLING NUISANCE VARIABLES

Our theoretical framework can handle *nuisance variables*, i.e., variables we cannot measure or perform weak supervision on. It may be impossible to label, or provide match-pairing on that factor of variation. For example, while many features of an image are measurable (such as brightness and coloration), we may not be able to measure certain factors of variation or generate data pairs where these factors are kept constant. In this case, we can let one additional variable η act as nuisance variable that captures all additional sources of variation / stochasticity.

Formally, suppose the full set of true factors is $S \cup \{\eta\} \in \mathbb{R}^{n+1}$. We define η-consistency $C_\eta(I) = C(I)$ and η-restrictiveness $R_\eta(I) = R(I \cup \{\eta\})$. This captures our intuition that, with nuisance variable, for consistency, we still want changes to $Z_{\setminus I} \cup \{\eta\}$ to not modify S_I; for restrictiveness, we want changes to $Z_I \cup \{\eta\}$ to only modify $S_I \cup \{\eta\}$. We define η-disentanglement as $D_\eta(I) = C_\eta(I) \wedge R_\eta(I)$.

All of our calculus still holds where we substitute $C_\eta(I), R_\eta(I), D_\eta(I)$ for $C(I), R(I), D(I)$; we prove one of the new full disentanglement rule as an illustration:

Theorem 2. $\bigwedge_{i=1}^n C_\eta(i) \iff \bigwedge_{i=1}^n D_\eta(i)$.

Proof. On the one hand, $\bigwedge_{i=1}^n C_\eta(i) \iff \bigwedge_{i=1}^n C(i) \implies C(1:n) \implies R(\eta)$. On the other hand, $\bigwedge_{i=1}^n C(i) \implies \bigwedge_{i=1}^n D(i) \implies \bigwedge_{i=1}^n R(i)$. Therefore $LHS \implies \forall i \in [n], R(i) \wedge R(\eta) \implies R_\eta(i)$. The reverse direction is trivial. □

In (Locatello et al., 2019), the "instance" factor in SmallNORB and the background image factor in Scream-dSprites are treated as nuisance variables. By Theorem 2, as long as we perform weak supervision on all of the non-nuisance variables (via sharing-pairing, say) to guarantee their consistency with respect to the corresponding true factor of variation, we still have guaranteed full disentanglement despite the existence of nuisance variable and the fact that we cannot measure or perform weak supervision on nuisance variable.

C SINGLE-FACTOR EXPERIMENTS

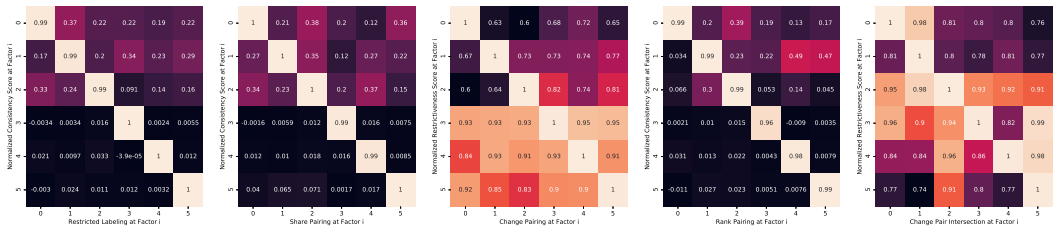

Figure 6: This is the same plot as Figure 6, but where we restrict our hyperparameter sweep to always set `extra dense = False`. See Appendix G for details about hyperparameter sweep.

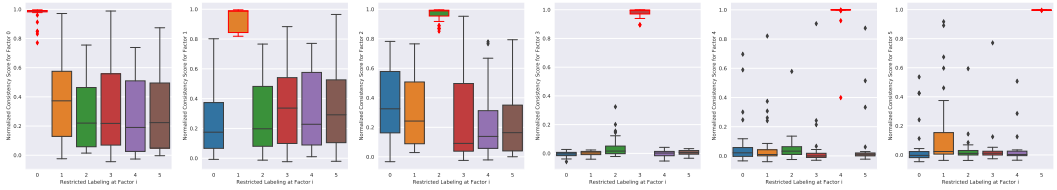

Figure 7: Restricted pairing guarantees consistency. Each plot shows the normalized consistency score of each model for each factor of variation. Our theory predicts each boxplot highlighted in red to achieve the highest consistency. Due to the prevalence of restricted pairing in the existing literature, we chose to only conduct the single-factor restricted labeling experiment on Shapes3D.

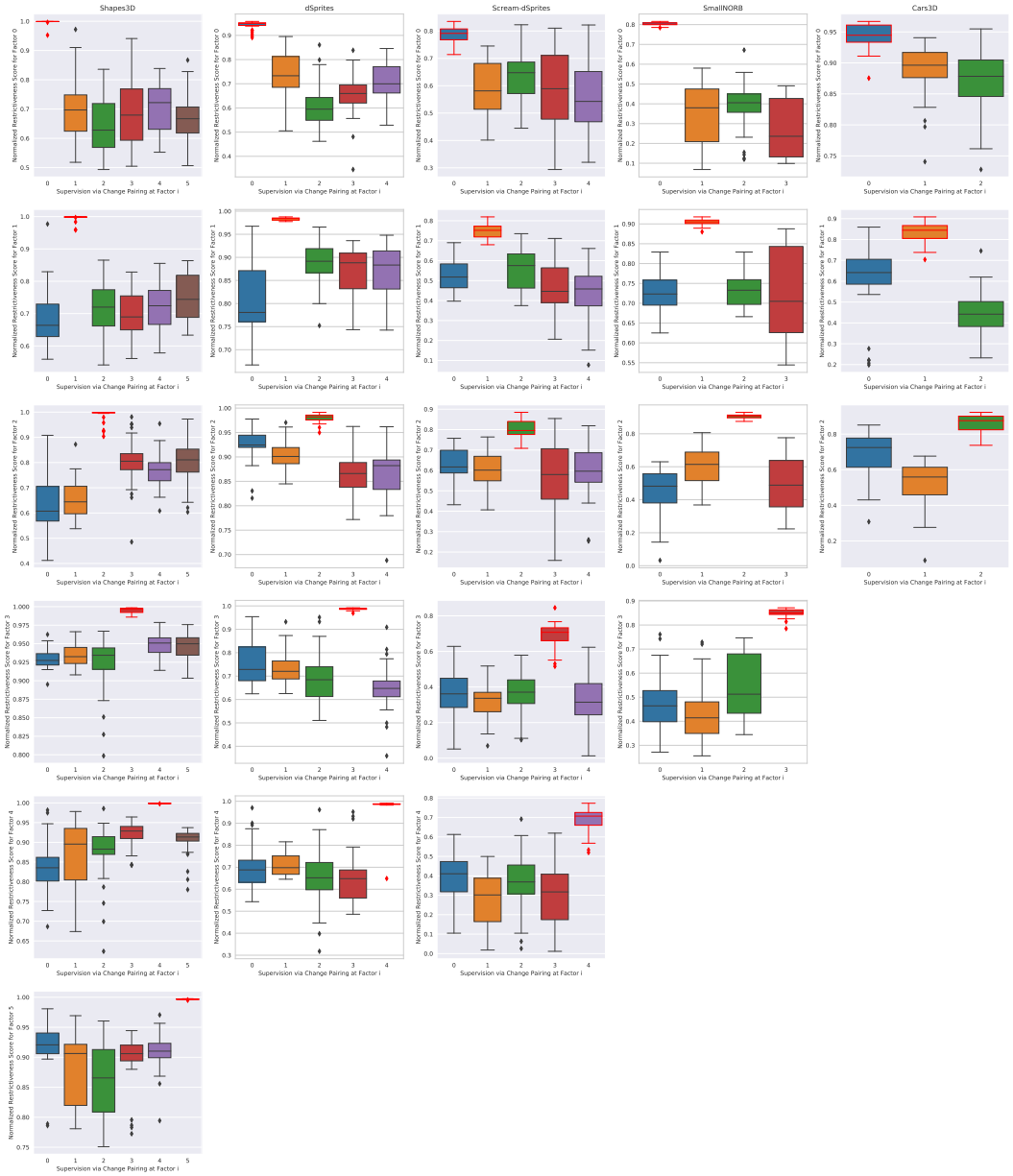

Figure 8: Change pairing guarantees restrictiveness. Each plot shows normalized restrictiveness score of each model for each factor of variation (row) across different datasets (columns). Different colors indicate models trained with change pairing on different factors. The appropriately-supervised model for each factor is marked in red.

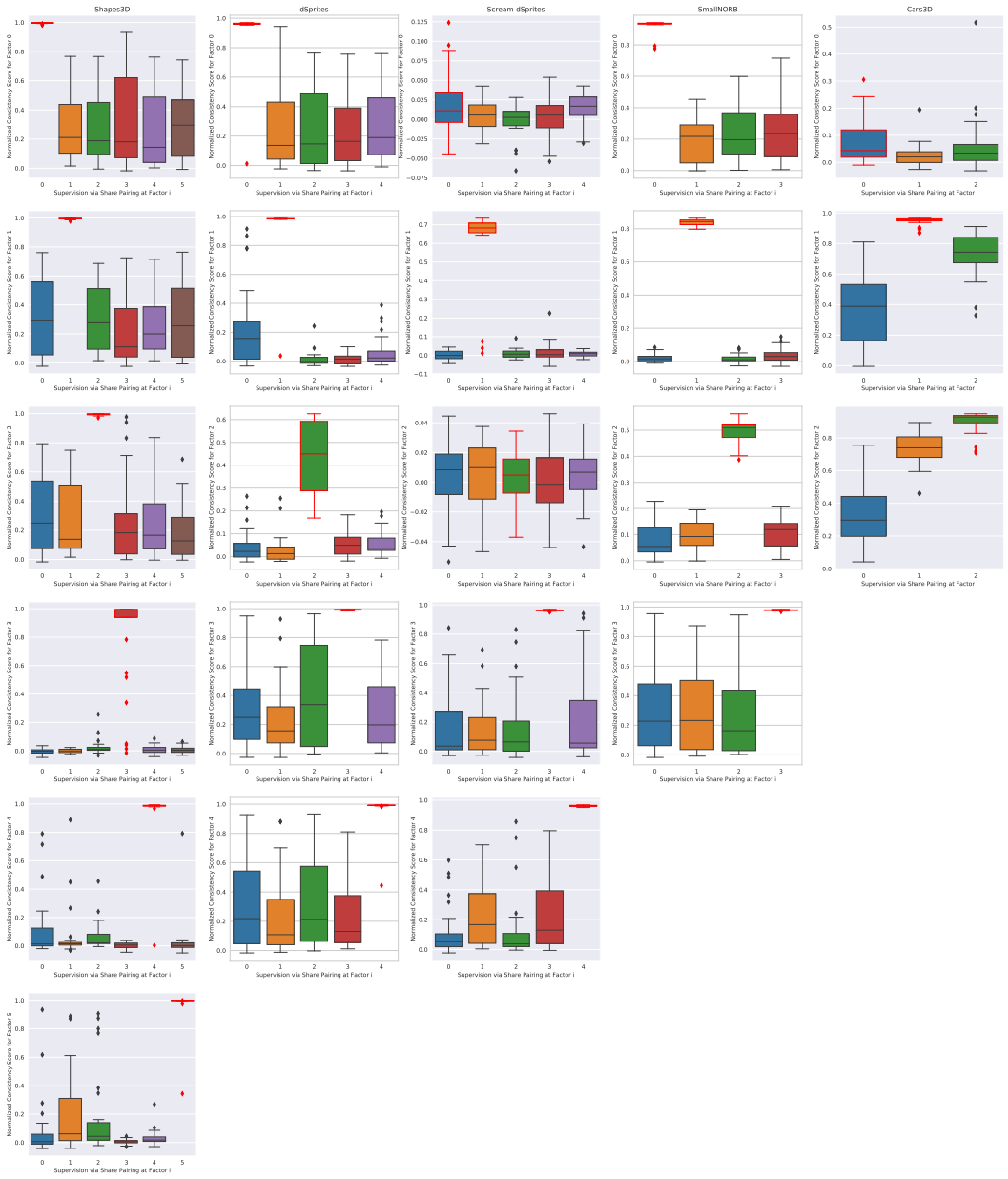

Figure 9: Share pairing guarantees consistency. Each plot shows normalized consistency score of each model for each factor of variation (row) across different datasets (columns). Different colors indicate models trained with share pairing on different factors. The appropriately-supervised model for each factor is marked in red.

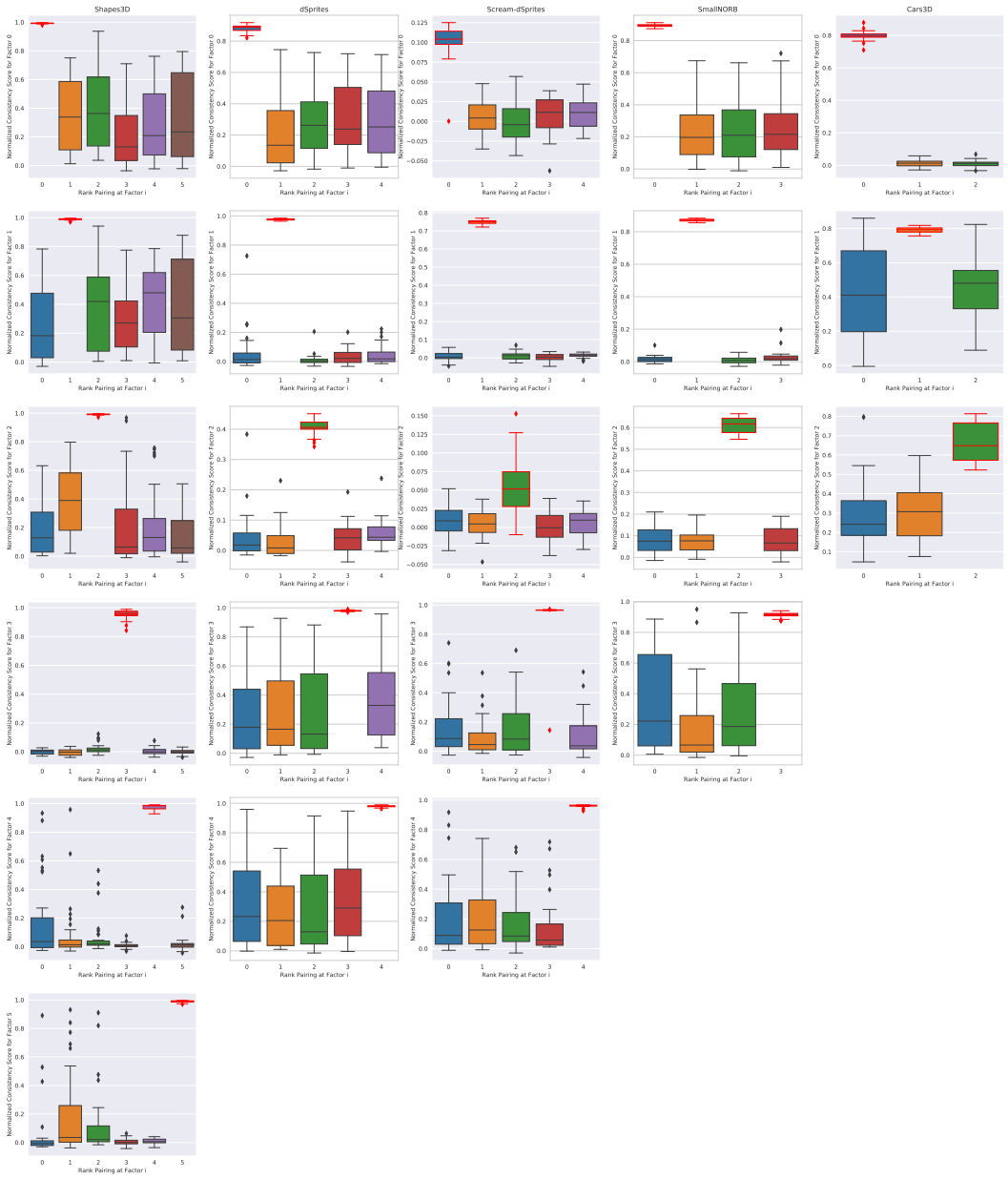

Figure 10: Rank pairing guarantees consistency. Each plot shows normalized consistency score of each model for each factor of variation (row) across different datasets (columns). Different colors indicate models trained with rank pairing on different factors. The appropriately-supervised model for each factor is marked in red.

D CONSISTENCY VERSUS RESTRICTIVENESS

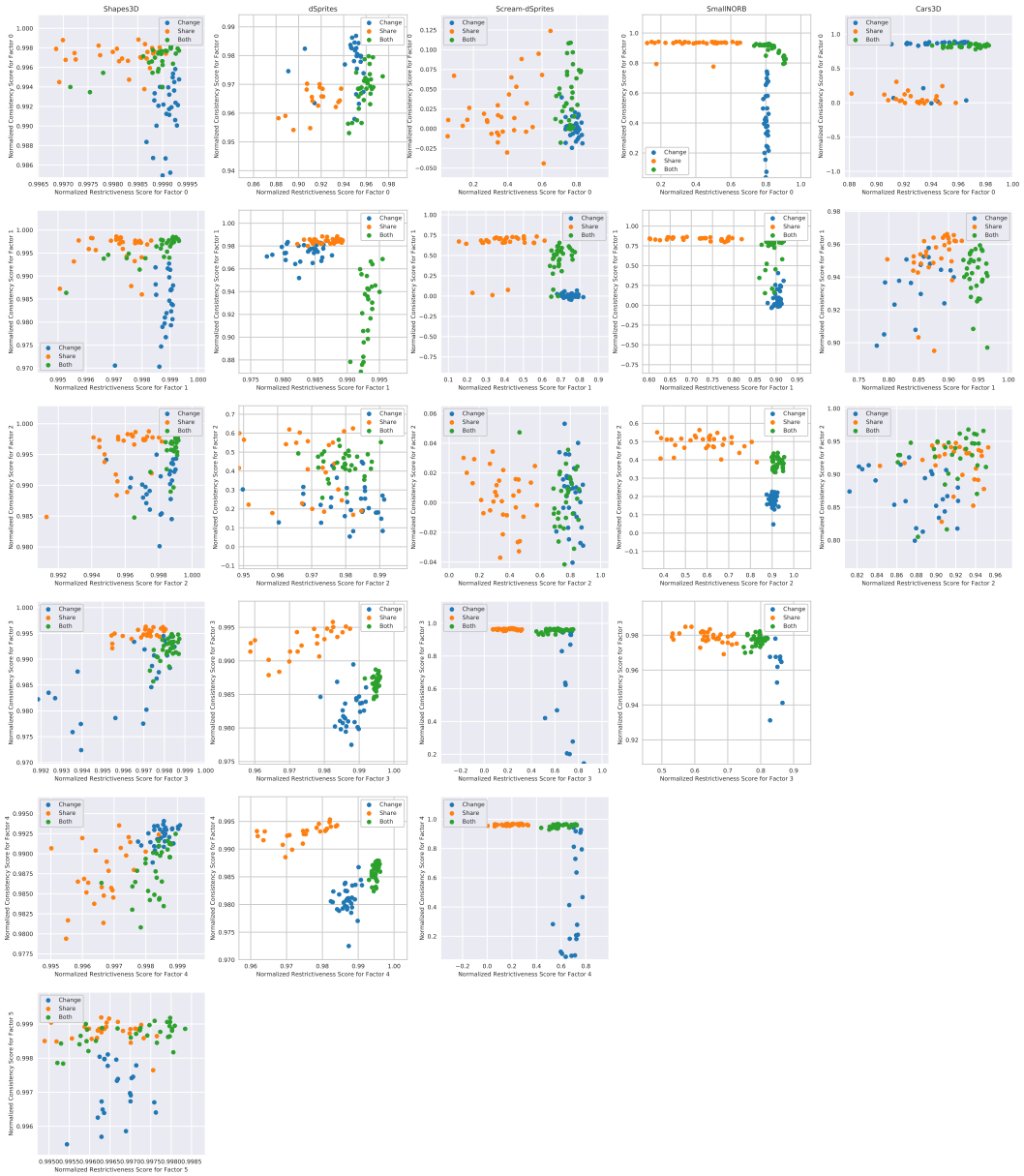

Figure 11: Normalized consistency vs. restrictiveness score of different models on each factor (row) across different datasets (columns). In many of the plots, we see that models trained via change-sharing (blue) achieve higher restrictiveness; models trained via share-sharing (orange) achieve higher consistency; models trained via both techniques (green) simultaneously achieve restrictiveness and consistency in most cases.

E FULL DISENTANGLEMENT EXPERIMENTS

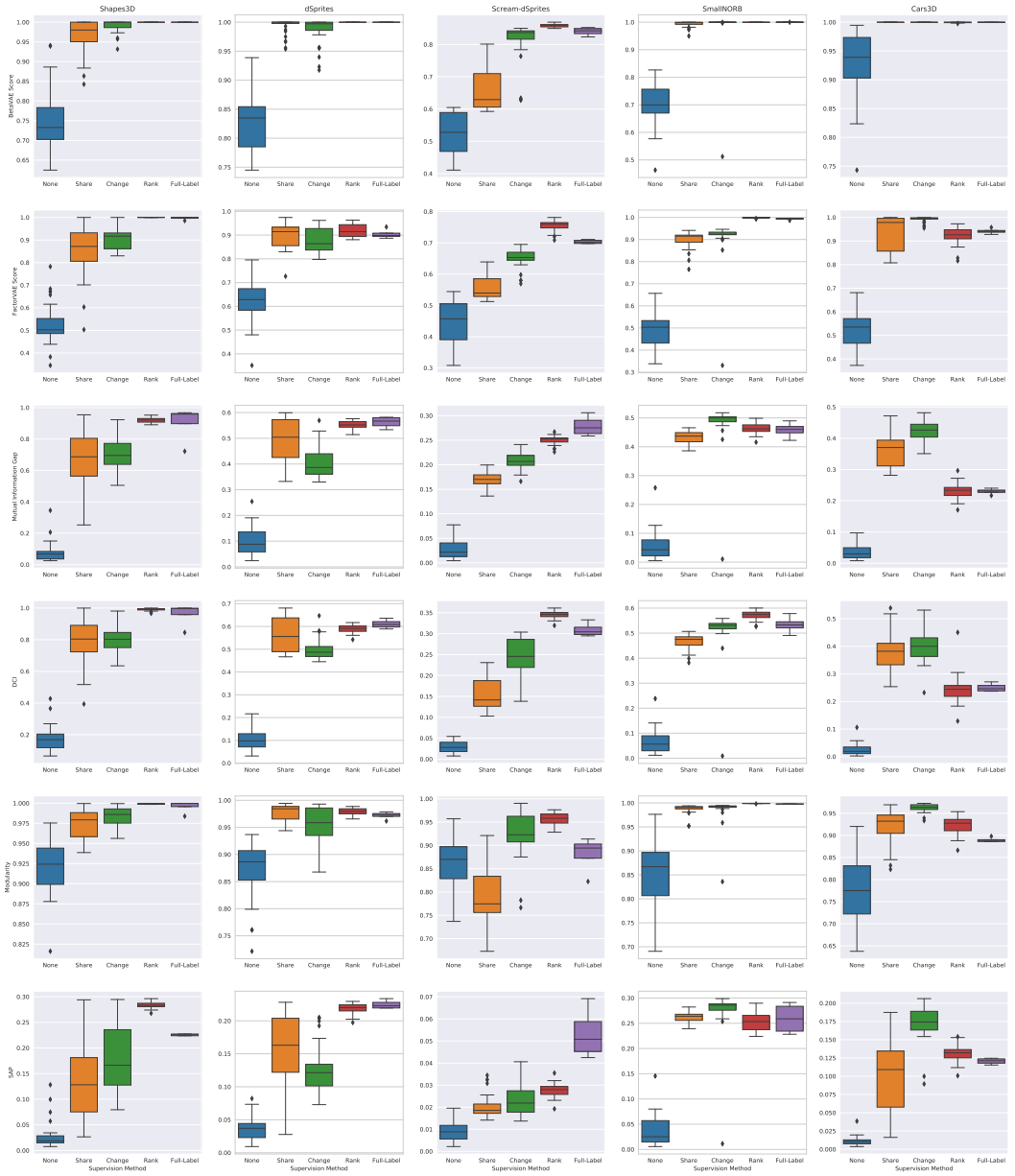

Figure 12: Disentanglement performance of a vanilla GAN, share pairing GAN, change pairing GAN, rank pairing GAN, and fully-labeled GAN, as measured by multiple disentanglement metrics in existing literature (rows) across multiple datasets (columns). According to almost all metrics, our weakly supervised models surpass the baseline, and in some cases, even outperform the fully-labeled model.

Figure 13: Performance of a vanilla GAN (blue), share pairing GAN (orange), change pairing GAN (green), rank pairing GAN (red), and fully-labeled GAN (purple), as measured by normalized consistency score of each factor (rows) across multiple datasets (columns). Factors $\{3, 4, 5\}$ in the first column shows that distribution matching to all six change / share pairing datasets is particularly challenging for the models when trained on certain hyperparameter choices. However, since consistency and restrictiveness can be measured in weakly supervised settings, it suffices to use these metrics for hyperparameter selection. We see in Figure 15 and Appendix F that using consistency and restrictiveness for hyperparameter selection serves as a viable weakly-supervised surrogate for existing fully-supervised disentanglement metrics.

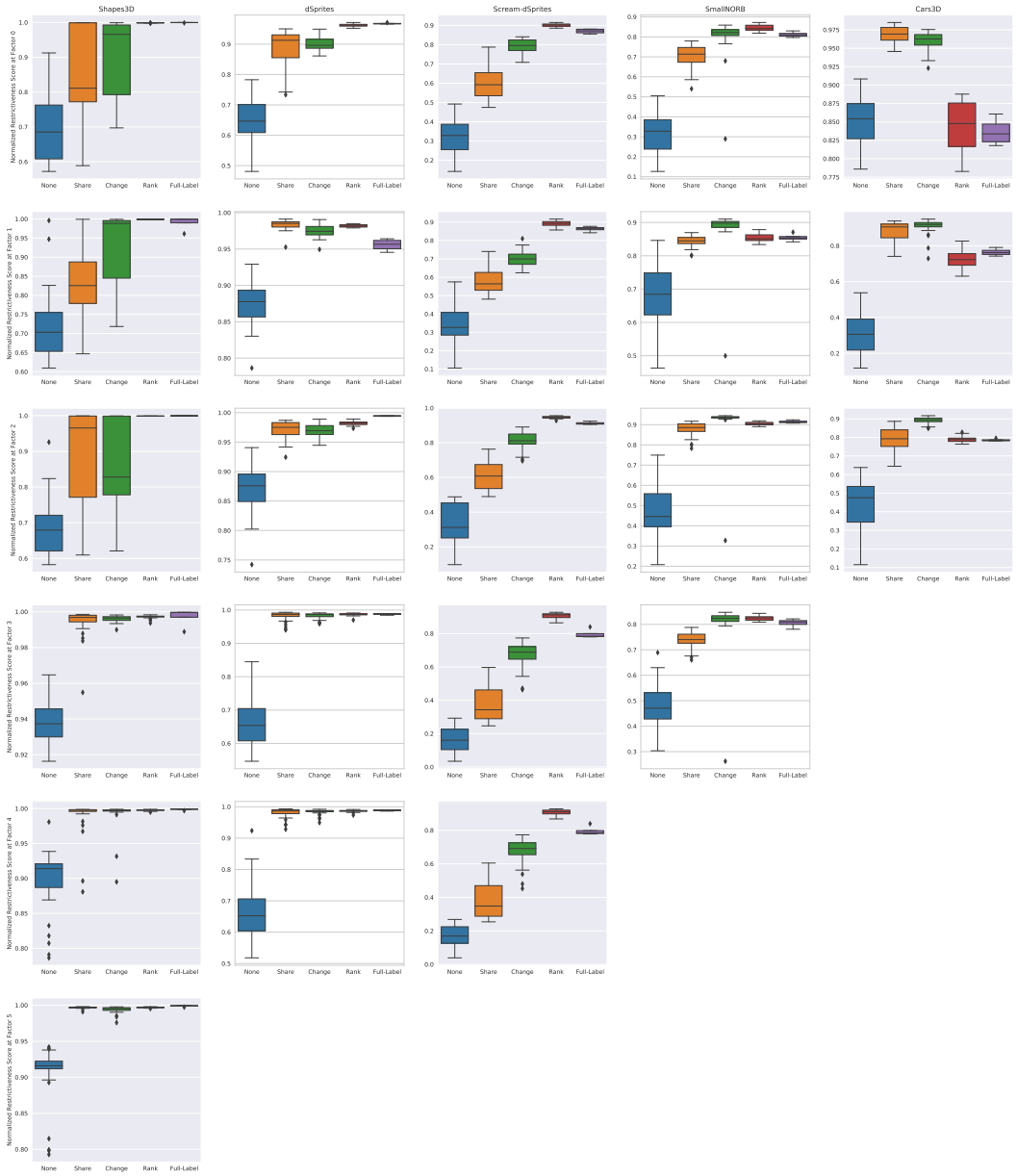

Figure 14: Performance of a vanilla GAN (blue), share pairing GAN (orange), change pairing GAN (green), rank pairing GAN (red), and fully-labeled GAN (purple), as measured by normalized restrictiveness score of each factor (rows) across multiple datasets (columns). Since restrictiveness and consistency are complementary, we see that the anomalies in Figure 13 are reflected in the complementary factors in this figure.

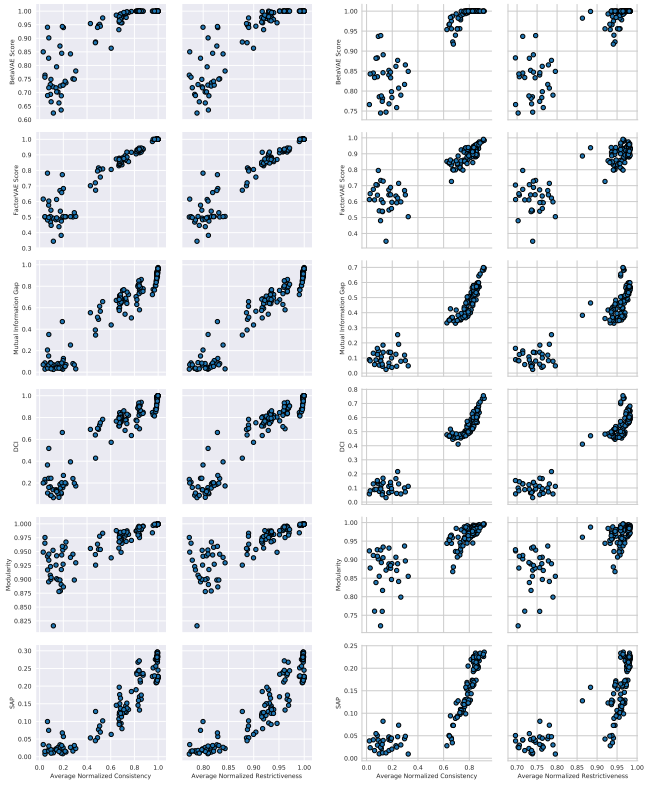

(a) Shapes3D

(b) dSprites

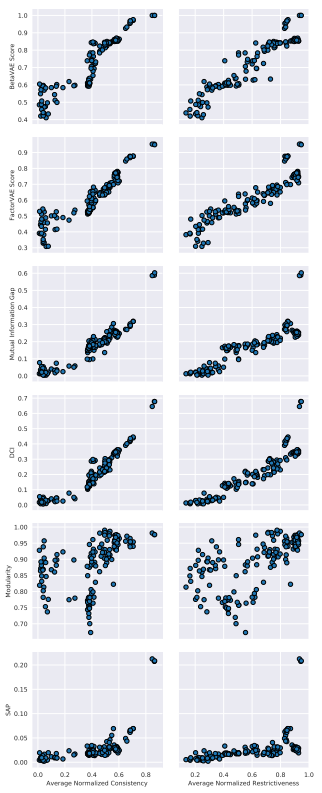

(c) Scream-dSprites

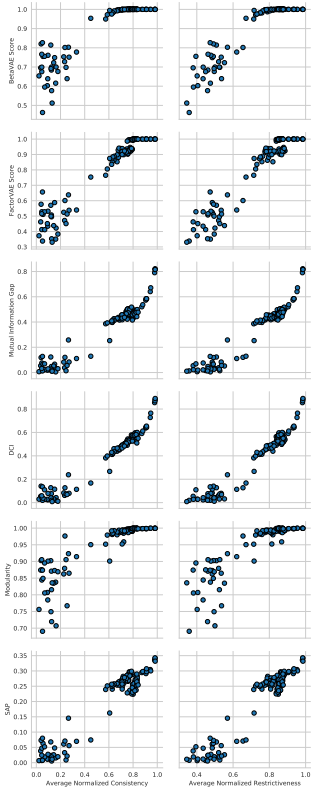

(d) SmallNORB

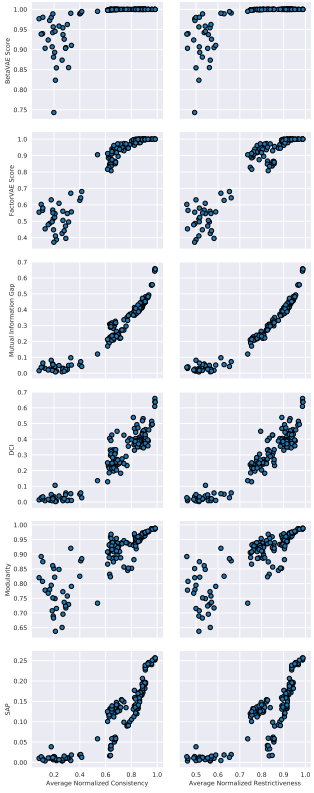

(e) Cars3D

Figure 15: Scatterplot of existing disentanglement metrics versus average normalized consistency and restrictiveness. Whereas existing disentanglement metrics are fully-supervised, it is possible to measure average normalized consistency and restrictiveness with weakly supervised data (share-pairing and match-pairing respectively), making it viable to perform hyperparameter tuning under weakly supervised conditions.

F FULL DISENTANGLEMENT VISUALIZATIONS

As a demonstration of the weakly-supervised generative models, we visualize our best-performing match-pairing generative models (as selected according to the normalized consistency score averaged across all the factors). Recall from Figures 2a to 2c that, to visually check for consistency and restrictiveness, it is important that we not only ablate a single factor (across the column), but also show that the factor stays consistent (down the row). Each block of 3×12 images in Figures 16 to 20 checks for disentanglement of the corresponding factor.

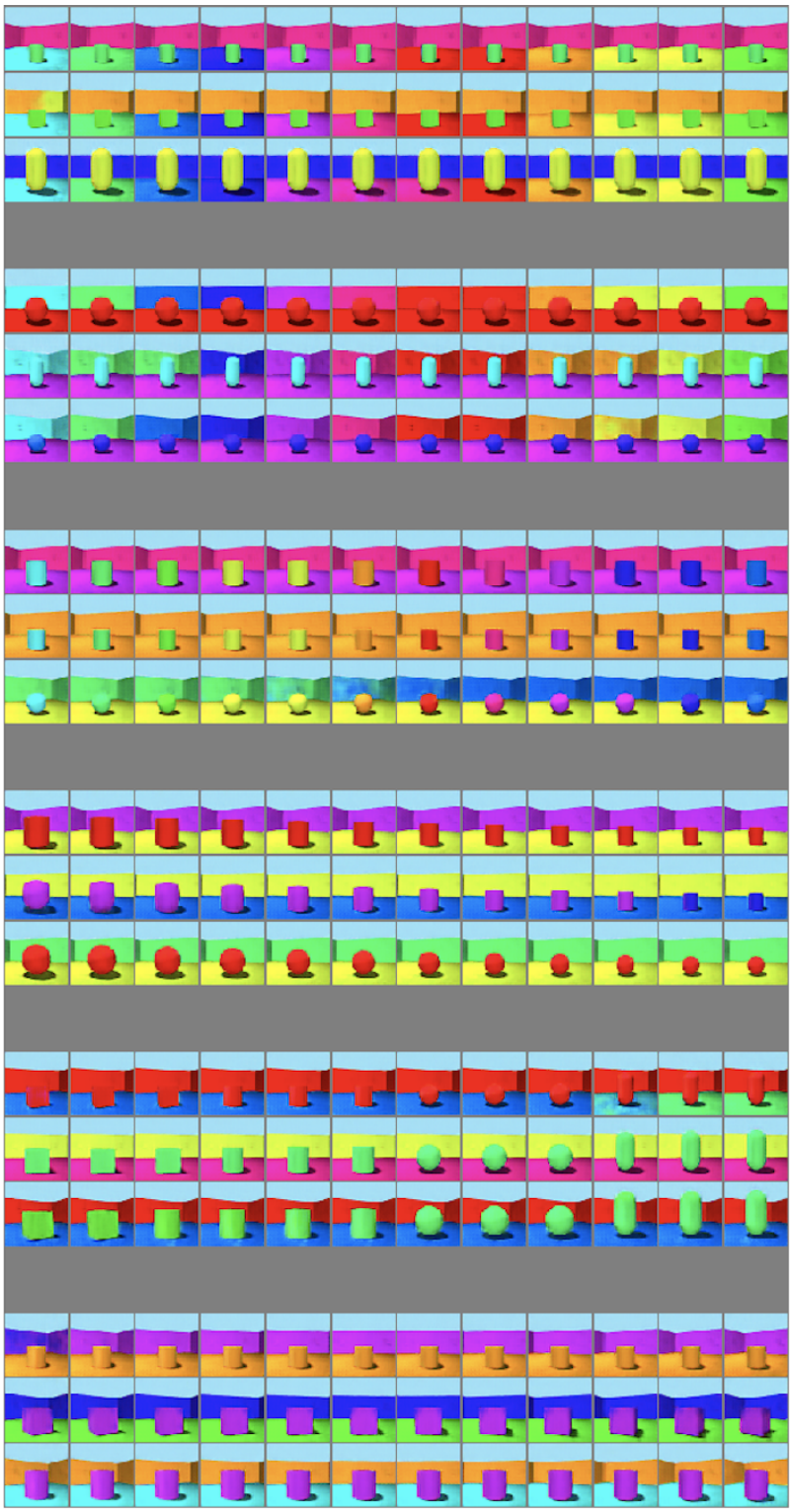

Figure 16: Shapes3D. Ground truth factors: floor color, wall color, object color, object size, object type, and azimuth.

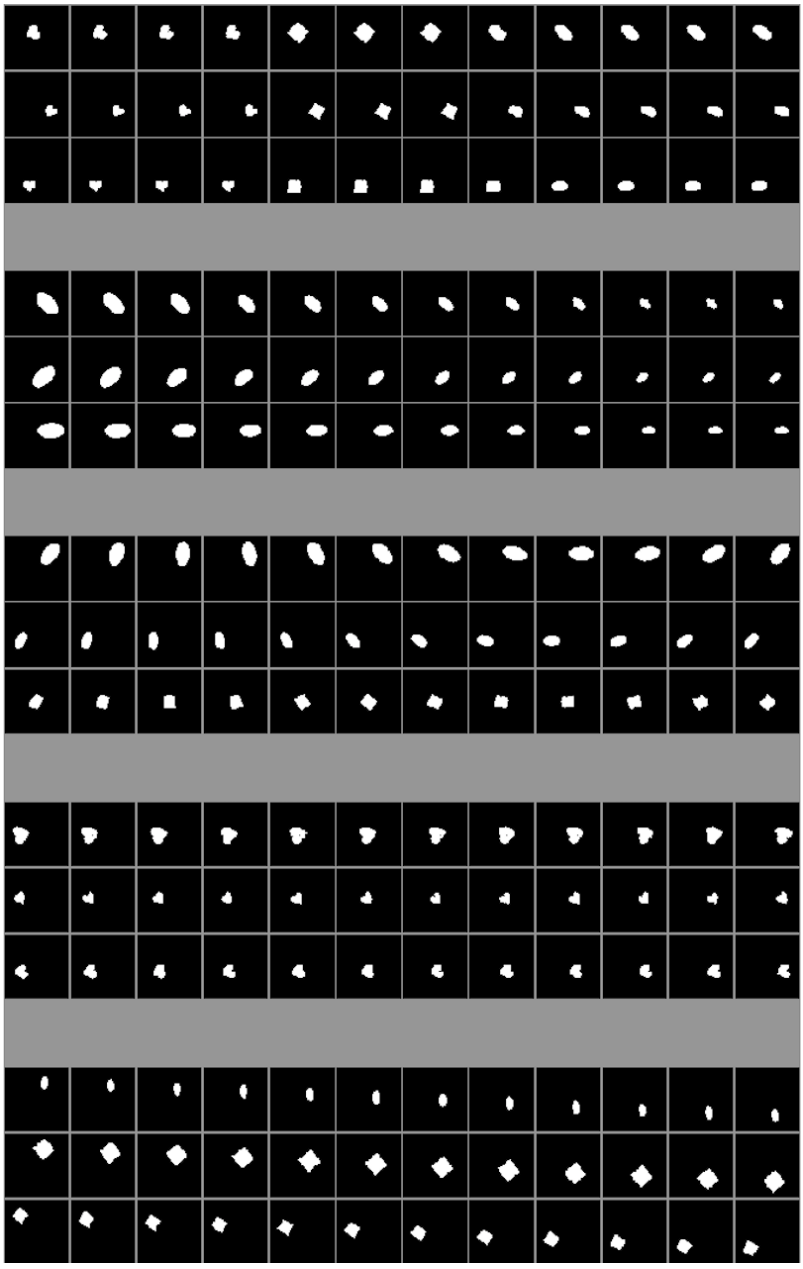

Figure 17: dSprites. Ground truth factors: shape, scale, orientation, X-position, Y-position.

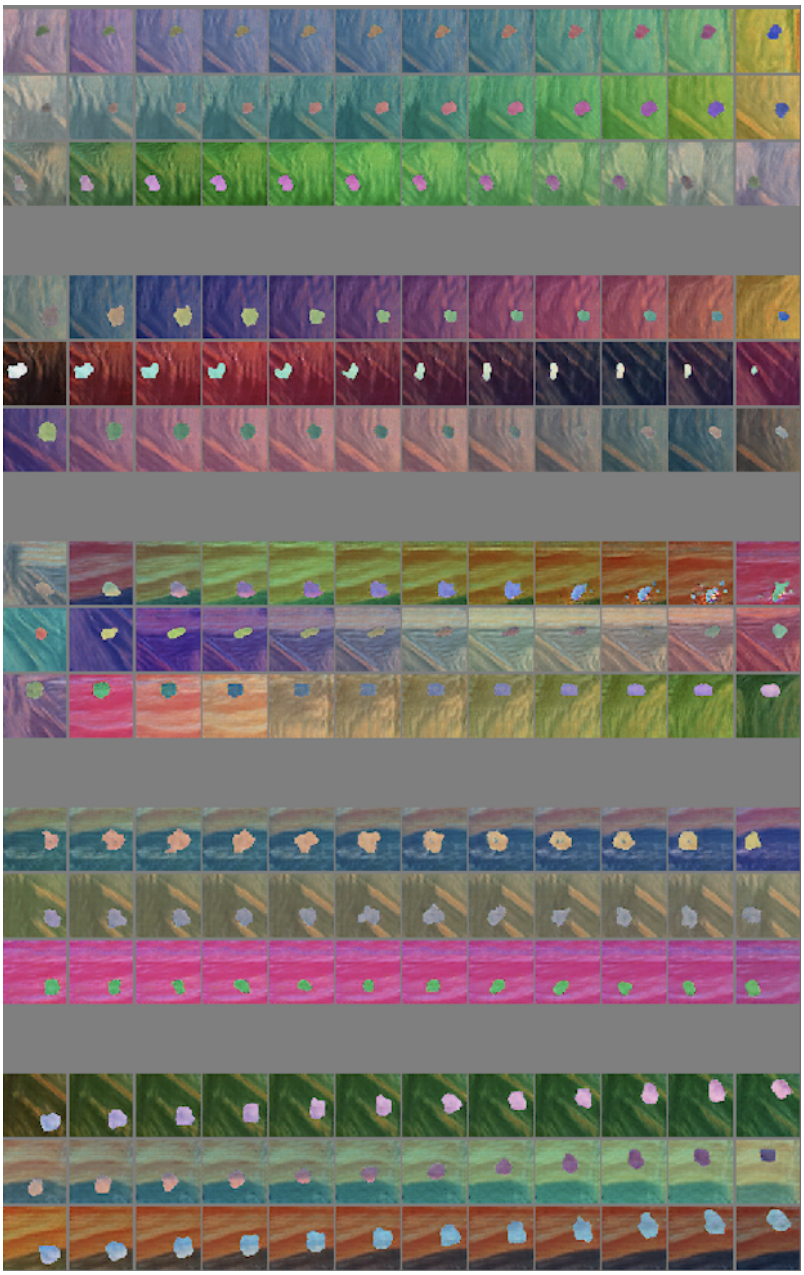

Figure 18: Scream-dSprites. Ground truth factors: shape, scale, orientation, X-position, Y-position.

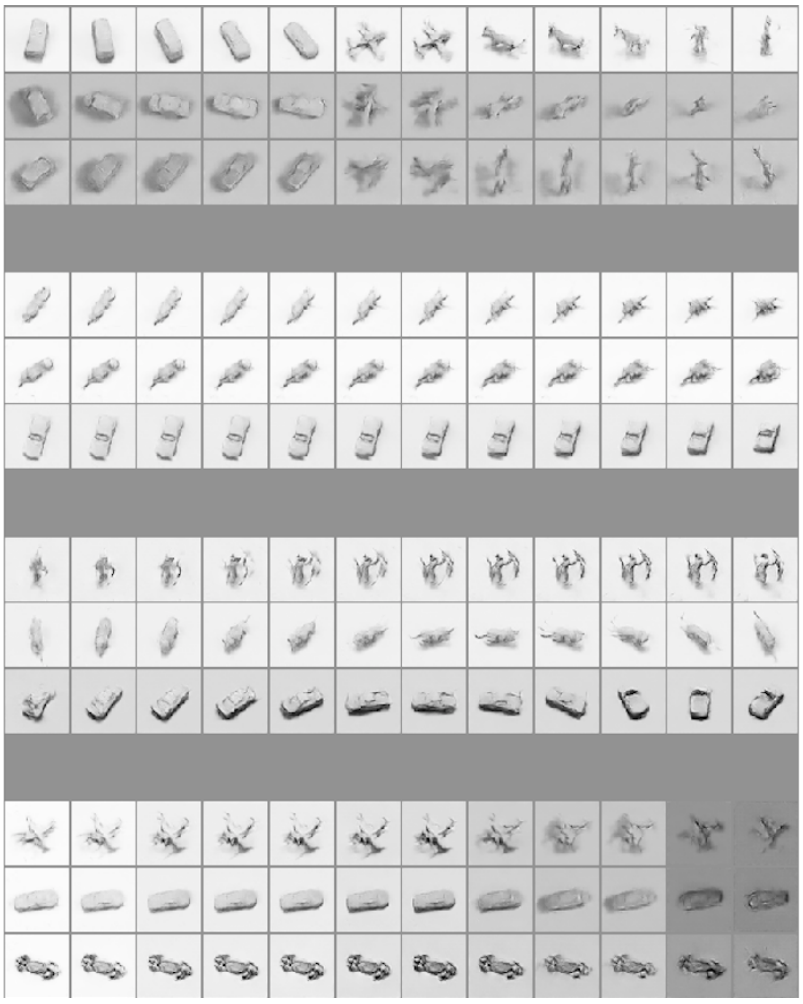

Figure 19: SmallNORB. Ground truth factors: category, elevation, azimuth, lighting condition.

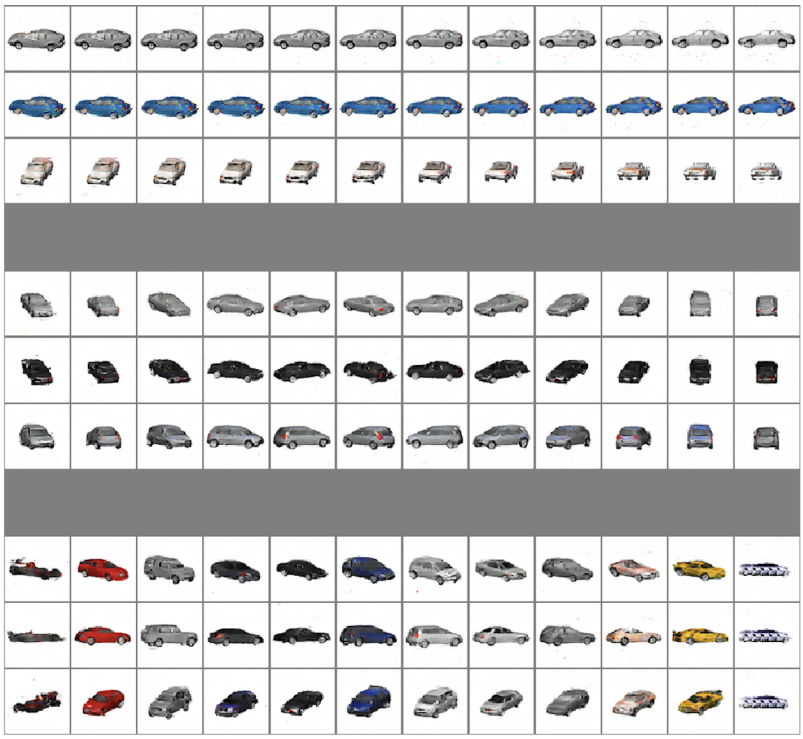

Figure 20: Cars3D. Ground truth factors: elevation, azimuth, object type.

G HYPERPARAMETERS

Table 1: We trained a probablistic Gaussian encoder to approximately invert the generative model. The encoder is not trained jointly with the generator, but instead trained separately from the generative model (i.e. encoder gradient does not backpropagate to generative model). During training, the encoder is only exposed to data generated by the learned generative model.

Encoder
4×4 spectral norm conv. 32. lReLU
4×4 spectral norm conv. 32. lReLU
4×4 spectral norm conv. 64. lReLU
4×4 spectral norm conv. 64. lReLU
flatten
128 spectral norm dense. lReLU
$2 \times z$-dim spectral norm dense

Table 2: Generative model architecture.

Generator
128 dense. ReLU. batchnorm.
1024 dense. ReLU. batchnorm.
$4 \times 4 \times 64$ reshape.
4×4 conv. 64. lReLU. batchnorm.
4×4 conv. 32. lReLU. batchnorm.
4×4 conv. 32. lReLU. batchnorm.
4×4 conv. 3. sigmoid

Table 3: Discriminator used for restricted labeling. Parts in red are part of hyperparameter search.

Discriminator Body
4×4 spectral norm conv. $32 \times$ width. lReLU
4×4 spectral norm conv. $32 \times$ width. lReLU
4×4 spectral norm conv. $64 \times$ width. lReLU
4×4 spectral norm conv. $64 \times$ width. lReLU
flatten
if extra dense: $128 \times$ width spectral norm dense. lReLU
Discriminator Auxiliary Channel for Label
$128 \times$ width spectral norm dense. lReLU
If extra dense: $128 \times$ width spectral norm dense. lReLU
Discriminator head
concatenate body and auxiliary.
$128 \times$ width spectral norm dense. lReLU
$128 \times$ width spectral norm dense. lReLU
1 spectral norm dense with bias.

Table 4: Discriminator used for match pairing. We use a projection discriminator (Miyato & Koyama, 2018) and thus have an unconditional and conditional head. Parts in red are part of hyperparameter search.

Discriminator Body Applied Separately to x and x'
4×4 spectral norm conv. $32 \times$ width. lReLU
4×4 spectral norm conv. $32 \times$ width. lReLU
4×4 spectral norm conv. $64 \times$ width. lReLU
4×4 spectral norm conv. $64 \times$ width. lReLU
flatten
If extra dense: $128 \times$ width spectral norm dense. lReLU
concatenate the pair.
$128 \times$ width spectral norm dense. lReLU
$128 \times$ width spectral norm dense. lReLU
Unconditional Head
1 spectral norm dense with bias
Conditional Head
$128 \times$ width spectral norm dense

Table 5: Discriminator used for rank pairing. For rank-pairing, we use a special variant of the projection discriminator, where the conditional logit is computed via taking the difference between the two pairs and multiplying by $y \in \{-1, +1\}$. The discriminator is thus implicitly taking on the role of an adversarially trained encoder that checks for violations of the ranking rule in the embedding space. Parts in red are part of hyperparameter search.

Discriminator Body Applied Separately to x and x'
4×4 spectral norm conv. $32 \times$ width. lReLU
4×4 spectral norm conv. $32 \times$ width. lReLU
4×4 spectral norm conv. $64 \times$ width. lReLU
4×4 spectral norm conv. $64 \times$ width. lReLU
flatten
If extra dense: $128 \times$ width spectral norm dense. lReLU
concatenate the pair.
Unconditional Head Applied Separately to x and x'
1 spectral norm dense with bias.
Conditional Head Applied Separately to x and x'
y-dim spectral norm dense.

For all models, we use the Adam optimizer with $\beta_1 = 0.5, \beta_2 = 0.999$ and set the generator learning rate to 1×10^{-3}. We use a batch size of 64 and set the leaky ReLU negative slope to 0.2.

To demonstrate some degree of robustness to hyperparameter choices, we considered five different ablations:

1. Width multiplier on the discriminator network ($\{1, 2\}$)
2. Whether to add an extra fully-connected layer to the discriminator ($\{\text{True}, \text{False}\}$).
3. Whether to add a bias term to the head ($\{\text{True}, \text{False}\}$).
4. Whether to use two-time scale learning rate by setting encoder+discriminator learning rate multipler to ($\{1, 2\}$).
5. Whether to use the default PyTorch or Keras initialization scheme in all models.

As such, each of our experimental setting trains a total of 32 *distinct* models. The only exception is the intersection experiments where we fixed the width multiplier to 1.[1]

To give a sense of the scale of our experimental setup, note that the 864 models in Figure 4 originate as follows:

1. 32 hyperparameter conditions $\times$ 6 restricted labeling conditions.
2. 32 hyperparameter conditions $\times$ 6 match pairing conditions.
3. 32 hyperparameter conditions $\times$ 6 share pairing conditions.
4. 32 hyperparameter conditions $\times$ 6 rank pairing conditions.
5. 16 hyperparameter conditions $\times$ 6 intersection conditions.

[1] Due to time constraints.

H PROOFS

H.1 ASSUMPTIONS ON $\mathcal{H}$

Assumption 1. Let $D \subseteq [n]$ indexes discrete random variables S_D. Assume that the remaining random variables $S_C = S_{\setminus D}$ have probability density function $p(s_C|s_D)$ for any set of values s_D where $p(S_D = s_D) > 0$.

Assumption 2. Without loss of generality, suppose $S_{1:n} = [S_C, S_D]$ is ordered by concatenating the continuous variables with the discrete variables. Let $\mathcal{B}(s_D) = [\text{int}(\text{supp}(p(s_C \mid s_D))), s_D]$ denote the interior of the support of the continuous conditional distribution of S_C concatenated with its conditioning variable s_D drawn from S_D. With a slight abuse of notation, let $\mathcal{B}(S) = \bigcup_{s_D : p(s_D > 0)} \mathcal{B}(s_D)$. We assume $\mathcal{B}(S)$ is *zig-zag connected*, i.e., for any $I, J \subseteq [n]$, for any two points $s_{1:n}, s'_{1:n} \in \mathcal{B}(S)$ that only differ in coordinates in $I \cup J$, there exists a path $\{s^t_{1:n}\}_{t=0:T}$ contained in $\mathcal{B}(S)$ such that

$$s^0_{1:n} = s_{1:n} \tag{12}$$

$$s^T_{1:n} = s'_{1:n} \tag{13}$$

$$\forall\, 0 \le t < T, \text{ either } s^t_{\setminus I} = s^{t+1}_{\setminus I} \text{ or } s^t_{\setminus J} = s^{t+1}_{\setminus J}, \tag{14}$$

Intuitively, this assumption allows transition from $s_{1:n}$ to $s'_{1:n}$ via a series of modifications that are only in I or only in J. Note that zig-zag connectedness is necessary for restrictiveness union (Theorem 4) and consistency intersection (Theorem 5). Fig. 21 gives examples where restrictiveness union is not satisfied when zig-zag connectedness is violated.

Assumption 3. For arbitrary coordinate $j \in [m]$ of g that maps to a continuous variable X_j, we assume that $g_j(s)$ is continuous at s, $\forall s \in \mathcal{B}(S)$; For arbitrary coordinate $j \in [m]$ of g that maps to a discrete variable X_j, $\forall s_D$ where $p(s_D) > 0$, we assume that $g_j(s)$ is constant over each connected component of $\text{int}(\text{supp}(p(s_C \mid s_D))$.

Define $\mathcal{B}(X)$ analogously to $\mathcal{B}(S)$. Symmetrically, for arbitrary coordinate $i \in [n]$ of e that maps to a continuous variable S_i, we assume that $e_i(x)$ is continuous at x, $\forall x \in \mathcal{B}(X)$; For arbitrary coordinate $i \in [n]$ of e that maps to a discrete S_i, $\forall x_D$ where $p(x_D) > 0$, we assume that $e_i(x)$ is constant over each connected component of $\text{int}(\text{supp}(p(x_C \mid x_D))$.

Assumption 4. Assume that every factor of variation is recoverable from the observation $\mathcal{X}$. Formally, (p, g, e) satisfies the following property

$$\mathbb{E}_{p(s_{1:n})} \| e \circ g(s_{1:n}) - s_{1:n} \|^2 = 0. \tag{15}$$

H.2 CALCULUS OF DISENTANGLEMENT

H.2.1 A USEFUL LEMMA

Lemma 1. *Let x, y be two random variables with distribution p, $f(x, y)$ be arbitrary function. Then*

$$\mathbb{E}_{x \sim p(x)} \mathbb{E}_{y, y' \sim p(y|x)} \| f(x, y) - f(x, y') \|^2 \le \mathbb{E}_{(x,y),(x',y') \sim p(x,y)} \| f(x, y) - f(x', y') \|^2.$$

Proof. Assume w.l.o.g that $\mathbb{E}_{(x,y) \sim p(x,y)} f(x, y) = 0$.

$$LHS = 2\mathbb{E}_{(x,y) \sim p(x,y)} \| f(x, y) \|^2 - 2\mathbb{E}_{x \sim p(x)} \mathbb{E}_{y, y' \sim p(y|x)} f(x, y)^T f(x, y') \tag{16}$$

$$= 2\mathbb{E}_{(x,y) \sim p(x,y)} \| f(x, y) \|^2 - 2\mathbb{E}_{x \sim p(x)} \mathbb{E}_{y \sim p(y|x)} f(x, y)^T \mathbb{E}_{y' \sim p(y|x)} f(x, y') \tag{17}$$

$$= 2\mathbb{E}_{(x,y) \sim p(x,y)} \| f(x, y) \|^2 - 2\mathbb{E}_{x \sim p(x)} \| \mathbb{E}_{y \sim p(y|x)} f(x, y) \|^2 \tag{18}$$

$$\le 2\mathbb{E}_{(x,y) \sim p(x,y)} \| f(x, y) \|^2 \tag{19}$$

$$= 2\mathbb{E}_{(x,y) \sim p(x,y)} \| f(x, y) \|^2 - 2\| \mathbb{E}_{(x,y) \sim p(x,y)} f(x, y) \|^2 \tag{20}$$

$$= 2\mathbb{E}_{(x,y) \sim p(x,y)} \| f(x, y) \|^2 - 2\mathbb{E}_{(x,y),(x',y') \sim p(x,y)} f(x, y)^T f(x', y') \tag{21}$$

$$= RHS. \tag{22}$$

□

H.2.2 CONSISTENCY UNION

Let $L = I \cap J$,$K = \setminus (I \cup J)$, $M = I - L$,$N = J - L$.

Theorem 3. $C(I) \wedge C(J) \implies C(I \cup J)$.

Proof.

$$C(I) \implies \mathbb{E}_{z_M, z_L} \mathbb{E}_{z_N, z'_N, z_K, z'_K} \| r_I \circ G(z_M, z_L, z_N, z_K) - r_I \circ G(z_M, z_L, z'_N, z'_K) \|^2 = 0. \tag{23}$$

For any fixed value of z_M, z_L,

$$\mathbb{E}_{z_N, z'_N, z_K, z'_K} \| r_I \circ G(z_M, z_L, z_N, z_K) - r_I \circ G(z_M, z_L, z'_N, z'_K) \|^2 \tag{24}$$

$$\geq \mathbb{E}_{z_N} \mathbb{E}_{z_K, z'_K} \| r_I \circ G(z_M, z_L, z_N, z_K) - r_I \circ G(z_M, z_L, z_N, z'_K) \|^2. \tag{25}$$

by plugging in $x = z_N$, $y = z_K$ into Lemma 1. Therefore

$$C(I) \implies \mathbb{E}_{z_M, z_L, z_N} \mathbb{E}_{z_K, z'_K} \| r_I \circ G(z_M, z_L, z_N, z_K) - r_I \circ G(z_M, z_L, z_N, z'_K) \|^2 = 0. \tag{26}$$

Similarly we have

$$C(J) \implies \mathbb{E}_{z_M, z_L, z_N} \mathbb{E}_{z_K, z'_K} \| r_J \circ G(z_M, z_L, z_N, z_K) - r_J \circ G(z_M, z_L, z_N, z'_K) \|^2 = 0 \tag{27}$$

$$\implies \mathbb{E}_{z_M, z_L, z_N} \mathbb{E}_{z_K, z'_K} \| r_N \circ G(z_M, z_L, z_N, z_K) - r_N \circ G(z_M, z_L, z_N, z'_K) \|^2 = 0. \tag{28}$$

As $I \cap N = \emptyset$, $I \cup N = I \cup J$, adding the above two equations gives us $C(I \cup J)$. □

H.2.3 RESTRICTIVENESS UNION

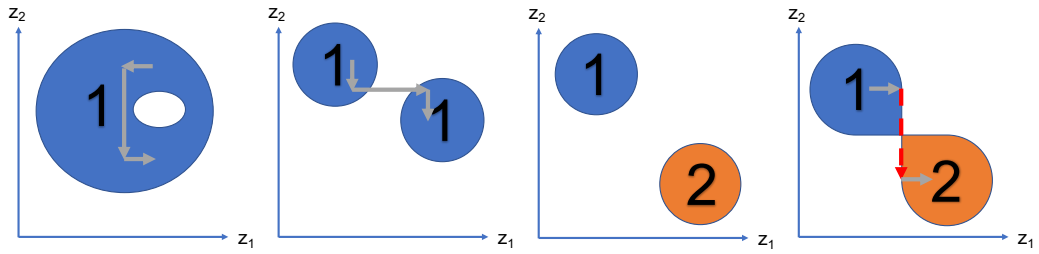

Figure 21: Zig-zag connectedness is necessary for restriveness union. Here $n = m = 3$. Colored areas indicate the support of $p(z_1, z_2)$; the marked numbers indicate the measurement of s_3 given (z_1, z_2). Left two panels satisfy zig-zag connectedness (the paths are marked in gray) while the right two do not (indeed $R(1) \wedge R(2) \nRightarrow R(\{1, 2\})$). In the right-most panel, any zig-zag path connecting two points from blue and orange areas has to pass through boundary of the support (disallowed).

Similarly define index sets L, K, M, N.

Theorem 4. *Under assumptions specified in Appendix H.1,* $R(I) \wedge R(J) \implies R(I \cup J)$.

Proof. Denote $f = e_K^* \circ g$. We claim that

$$R(I) \iff \mathbb{E}_{z_{\setminus I}} \mathbb{E}_{z_I, z'_I} \| f(z_I, z_{\setminus I}) - f(z'_I, z_{\setminus I}) \|^2 = 0. \tag{29}$$

$$\iff \forall (z_I, z_{\setminus I}), (z'_I, z_{\setminus I}) \in \mathcal{B}(Z), f(z_I, z_{\setminus I}) = f(z'_I, z_{\setminus I}). \tag{30}$$

We first prove the backward direction: When we draw $z_{\setminus I} \sim p(z_{\setminus I}), z_I, z'_I \sim p(z_I | z_{\setminus I})$, let E_1 denote the event that $(z_I, z_{\setminus I}) \notin \mathcal{B}(Z)$, and E_2 denote the event that $(z'_I, z_{\setminus I}) \notin \mathcal{B}(Z)$. Reorder the indices of $(z_I, z_{\setminus I})$ as (z_C, z_D). The probability that $(z_I, z_{\setminus I}) \notin \mathcal{B}(Z)$ (i.e.,z_C is on the boundary of $\mathcal{B}(z_D)$) is 0. Therefore $\Pr[E_1] = \Pr[E_2] = 0$. Therefore $\Pr[E_1 \cup E_2] \leq \Pr[E_1] + \Pr[E_2] = 0$, i.e., with probability 1, $\| f(z_I, z_{\setminus I}) - f(z'_I, z_{\setminus I}) \|^2 = 0$.

Now we prove the forward direction: Assume for the sake of contradiction that $\exists(z_I, z_{\setminus I}), (z'_I, z_{\setminus I}) \in \mathcal{B}(Z)$ such that $f(z_I, z_{\setminus I}) < f(z'_I, z_{\setminus I})$. Denote $U = I \cap D$, $V = I \cap C$, $W = \setminus I \cap D$, $Q = \setminus I \cap C$. We have $f(z_U, z_V, z_W, z_Q) < f(z'_U, z'_V, z_W, z_Q)$. Since f is continuous (or constant) at (z_U, z_V, z_W, z_Q) in the interior of $\mathcal{B}([z_U, z_W])$, and f is also continuous (or constant) at (z'_U, z'_V, z_W, z_Q) in the interior of $\mathcal{B}([z'_U, z_W])$, we can draw open balls of radius $r > 0$ around each point, i.e., $B_r(z_V, z_Q) \subset \mathcal{B}([z_U, z_W])$ and $B_r(z'_V, z_Q) \subset \mathcal{B}([z'_U, z_W])$, where

$$\forall(z^*_V, z^*_Q) \in B_r(z_V, z_Q), \forall(z^\Delta_V, z^\Delta_Q) \in B_r(z'_V, z_Q), f(z_U, z^*_V, z_W, z^*_Q) < f(z'_U, z^\Delta_V, z_W, z^\Delta_Q). \tag{31}$$

When we draw $z_{\setminus I} \sim p(z_{\setminus I}), z_I, z'_I \sim p(z_I|z_{\setminus I})$, let C denote the event that $(z_I, z_{\setminus I}) = (z^*_V, z_U, z^\#_Q, z_W)$, $(z'_I, z_{\setminus I}) = (z^\Delta_V, z'_U, z^\#_Q, z_W)$ where $(z^*_V, z^\#_Q) \in B_r(z_V, z_Q)$ and $(z^\Delta_V, z^\#_Q) \in B_r(z'_V, z_Q)$. Since both balls have positive volume, $\Pr[C] > 0$. However, $\|f(z_I, z_{\setminus I}) - f(z'_I, z_{\setminus I})\|^2 > 0$ whenever event C happens, which contradicts $R(I)$. Therefore $\forall(z_I, z_{\setminus I}), (z'_I, z_{\setminus I}) \in \mathcal{B}(Z), f(z_I, z_{\setminus I}) = f(z'_I, z_{\setminus I})$.

We have shown that

$$R(I) \iff \forall(z_M, z_L, z_N, z_K), (z'_M, z'_L, z_N, z_K) \in \mathcal{B}(Z), f(z_M, z_L, z_N, z_K) = f(z'_M, z'_L, z_N, z_K). \tag{32}$$

Similarly

$$R(J) \iff \forall(z_M, z_L, z_N, z_K), (z_M, z'_L, z'_N, z_K) \in \mathcal{B}(Z), f(z_M, z_L, z_N, z_K) = f(z_M, z'_L, z'_N, z_K). \tag{33}$$

$$R(I \cup J) \iff \forall(z_M, z_L, z_N, z_K), (z'_M, z'_L, z'_N, z_K) \in \mathcal{B}(Z), f(z_M, z_L, z_N, z_K) = f(z'_M, z'_L, z'_N, z_K) \tag{34}$$

Let the zig-zag path between (z_M, z_L, z_N, z_K) and $(z'_M, z'_L, z'_N, z_K) \in \mathcal{B}(Z)$ be $\{(z^t_M, z^t_L, z^t_N, z_K)\}_{t=0}^T$. Repeatedly applying the equivalent conditions of $R(I)$ and $R(J)$ gives us

$$f(z_M, z_L, z_N, z_K) = f(z^1_M, z^1_L, z^1_N, z_K) = \cdots = f(z^{T-1}_M, z^{T-1}_L, z^{T-1}_N, z_K) = f(z'_M, z'_L, z'_N, z_K). \tag{35}$$

□

H.3 Consistency and Restiveness Intersection

Theorem 5. *Under the same assumptions as restrictiveness union,* $C(I) \wedge C(J) \implies C(I \cap J)$.

Proof.

$$\begin{aligned} C(I) \wedge C(J) &\implies R(\setminus I) \wedge R(\setminus J) && (36)\\ &\implies R(\setminus I \cup \setminus J) && (37)\\ &\implies C(\setminus(\setminus I \cup \setminus J)) && (38)\\ &\implies C(I \cap J). && (39) \end{aligned}$$

□

Theorem 6. $R(I) \wedge R(J) \implies R(I \cap J)$.

Proof is analogous to Theorem 5.

H.4 Distribution matching guarantees latent code informativeness

Theorem 7. *If* $(p^*, g^*, e^*) \in \mathcal{H}$, *and* $(p, g, e) \in \mathcal{H}$, *and* $g^*(S) \overset{d}{=} g(Z)$, *then there exists a continuous function* r *such that*

$$\mathbb{E}_{p(s_{1:n})} \|r \circ e \circ g^*(s) - s\| = 0. \tag{40}$$

Proof. We show that $r = e^* \circ g$ satisfies Theorem 7. By Assumption 4,

$$\mathbb{E}_s \|e^* \circ g^*(s) - s\|^2 = 0. \tag{41}$$

$$\mathbb{E}_z \|e \circ g(z) - z\|^2 = 0. \tag{42}$$

By the same reasoning as in the proof of Theorem 4,

$$\mathbb{E}_s \|e^* \circ g^*(s) - s\|^2 = 0 \implies \forall s \in \mathcal{B}(S), e^* \circ g^*(s) = s. \tag{43}$$

$$\mathbb{E}_z \|e \circ g(z) - z\|^2 = 0 \implies \forall z \in \mathcal{B}(Z), e \circ g(z) = z. \tag{44}$$

Let $s \sim p(s)$. We claim that $\Pr[E_1] = 1$, where E_1 denote the event that $\exists z \in \mathcal{B}(Z)$ such that $g^*(s) = g(z)$. Suppose to the contrary that there is a measure-non-zero set $\mathcal{S} \subseteq supp(p(s))$ such that $\forall s \in \mathcal{S}$, no $z \in \mathcal{B}(Z)$ satisfies $g^*(s) = g(z)$. Let $\mathcal{X} = \{g(s) : s \in \mathcal{S}\}$. As $g^*(S) \overset{d}{=} g(Z)$, $\Pr_s[g^*(s) \in \mathcal{X}] = \Pr_z[g(z) \in \mathcal{X}] > 0$. Therefore $\exists \mathcal{Z} \subseteq supp(p(z)) - \mathcal{B}(Z)$ such that $\mathcal{X} \subseteq \{g(z) : z \in \mathcal{Z})\}$. But $supp(p(z)) - \mathcal{B}(Z)$ has measure 0. Contradiction.

When we draw s, let E_2 denote the event that $s \in \mathcal{B}(S)$. $\Pr[E_2] = 1$, so $\Pr[E_1 \wedge E_2] = 1$. When $E_1 \wedge E_2$ happens, $e^* \circ g \circ e \circ g^*(s) = e^* \circ g \circ e \circ g(z) = e^* \circ g(z) = e^* \circ g^*(s) = s$. Therefore

$$\mathbb{E}_s \|e^* \circ g \circ e \circ g^*(s) - s\| = 0. \tag{45}$$

□

H.5 Theorem 1: Restricted Labeling guarantees consistency

Theorem 8. *Given any oracle $(p^*(s_{1:n}), g^*, e^*) \in \mathcal{H}$, consider the distribution-matching algorithm $\mathcal{A}$ that selects a model $(p(z_{1:n}), g, e) \in \mathcal{H}$ such that $(g^*(S_{1:n}), S_I) \overset{d}{=} (g(Z_{1:n}), Z_I)$. Then g satisfies $C(I\,; p, g, e^*)$ and e satisfies $C(I\,; p^*, g^*, e)$.*

Proof. Since $(x_d, s_I) \overset{d}{=} (x_g, z_I)$, consider the measurable function

$$f(a, b) = \|e_I^*(a) - b\|^2. \tag{46}$$

We have

$$\mathbb{E}\|e_I^*(x_d) - s_I\|^2 = \mathbb{E}\|e_I^*(x_g) - z_I\|^2 = 0. \tag{47}$$

By the same reasoning as in the proof of Theorem 4,

$$\mathbb{E}_z \|e_I^* \circ g(z) - z_I\|^2 = 0 \implies \forall z \in \mathcal{B}(Z), e_I^* \circ g(z) = z_I. \tag{48}$$

Therefore

$$\mathbb{E}_{z_I} \mathbb{E}_{z_{\setminus I}, z'_{\setminus I}} \|e_I^* \circ g(z_I, z_{\setminus I}) - e_I^* \circ g(z_I, z'_{\setminus I})\|^2 = 0. \tag{49}$$

i.e., g satisfies $C(I\,; p, g, e^*)$. By symmetry, e satisfies $C(I\,; p^*, g^*, e)$. □

H.6 Restricted Labeling of s_I does not guarantee restrictiveness of z_I

Theorem 9. *Weak supervision via labeling of s_I is not sufficient for learning a generative model whose latent code z_I is restricted to s_I.*

Proof. We construct the following counterexample. Let $n = m = 3$ and $I = \{1\}$. The data generation process is $s_1 \sim unif([0, 2\pi))$, $(s_2, s_3) \sim unif(\{(x, y) : x^2 + y^2 <= 1\})$, $g^*(s) = [s_1, s_2, s_3]$. Consider a generator $z_1 \sim unif([0, 2\pi))$, $(s_2, s_3) \sim unif(\{(x, y) : x^2 + y^2 <= 1\})$, $g(z) = [z_1, \cos(z_1)z_2 - \sin(z_1)z_3, \sin(z_1)z_2 + \cos(z_1)z_3]$. Then $(x_d, s_I) \overset{d}{=} (x_g, z_I)$ but $R(I; p, g, e^*)$ does not hold. □

H.7 THEOREM 1: MATCH PAIRING GUARANTEES CONSISTENCY

Theorem 10. *Given any oracle $(p^*(s_{1:n}), g^*, e^*) \in \mathcal{H}$, consider the distribution-matching algorithm $\mathcal{A}$ that selects a model $(p(z_{1:n}), g, e) \in \mathcal{H}$ such that*

$$\left(g^*(S_I, S_{\setminus I}), g^*(S_I, S'_{\setminus I})\right) \stackrel{d}{=} \left(g(Z_I, Z_{\setminus I}), g(Z_I, Z'_{\setminus I})\right). \tag{50}$$

Then g satisfies $C(I\,;p,g,e^*)$ and e satisfies $C(I\,;p^*,g^*,e)$.

Proof.

$$\left(g^*(S_I, S_{\setminus I}), g^*(S_I, S'_{\setminus I})\right) \stackrel{d}{=} \left(g(Z_I, Z_{\setminus I}), g(Z_I, Z'_{\setminus I})\right) \tag{51}$$

$$\implies \|e_I^* \circ g^*(S_I, S_{\setminus I}) - e_I^* \circ g^*(S_I, S'_{\setminus I})\|^2 \stackrel{d}{=} \|e_I^* \circ g(Z_I, Z_{\setminus I}) - e_I^* \circ g(Z_I, Z'_{\setminus I})\|^2 \tag{52}$$

$$\implies \mathbb{E}_{z_I}\mathbb{E}_{z_{\setminus I}, z'_{\setminus I}}\|e_I^* \circ g(z_I, z_{\setminus I}) - e_I^* \circ g(z_I, z'_{\setminus I})\|^2 = 0. \tag{53}$$

So g satisfies $C(I\,;p,g,e^*)$. By symmetry, e satisfies $C(I\,;p^*,g^*,e)$. □

H.8 THEOREM 1: RANK PAIRING GUARANTEES CONSISTENCY

Theorem 11. *Given any oracle $p^*(s_{1:n}, g^*, e^*) \in \mathcal{H}$, consider the distribution-matching algorithm $\mathcal{A}$ that selects a model $(p(z_{1:n}), g, e) \in \mathcal{H}$ such that*

$$(g^*(S_{1:n}), g^*(S'_{1:n}), \mathbf{1}\{S_i \le S'_i\}) \stackrel{d}{=} (g(Z_{1:n}), g(Z'_{1:n}), \mathbf{1}\{Z_i \le Z'_i\}). \tag{54}$$

Then g satisfies $C(i\,;p,g,e^*)$ and e satisfies $C(i\,;p^*,g^*,e)$.

Proof. Let $I = \{i\}$, $f = e_I^* \circ g$. Distribution matching implies that, with probability 1 over random draws of Z, Z', the following event P happens:

$$Z_I <= Z'_I \implies f(Z) <= f(Z'). \tag{55}$$

i.e.,

$$\mathbb{E}_{z,z'}\mathbf{1}[\neg P] = 0. \tag{56}$$

Let $W = \setminus I \cap D$, $Q = \setminus I \cap \setminus D$. We showed in the proof of Theorem 4 that

$$C(I) \iff \forall (z_I, z_W, z_Q), (z_I, z'_W, z'_Q) \in \mathcal{B}(Z), f(z_I, z_W, z_Q) = f(z_I, z'_W, z'_Q). \tag{57}$$

We prove by contradiction. Suppose $\exists (z_I, z_W, z_Q), (z_I, z'_W, z'_Q) \in \mathcal{B}(Z)$ such that $f(z_I, z_W, z_Q) < f(z_I, z'_W, z'_Q)$.

1. Case 1: Z_I is discrete.

   Since f is constant both at (z_I, z_W, z_Q) in the interior of $\mathcal{B}([z_I, z_W])$, and at (z_I, z'_W, z'_Q) in the interior of $\mathcal{B}([z_I, z'_W])$, we can draw open balls of radius $r > 0$ around each point, i.e., $B_r(z_Q) \subset \mathcal{B}([z_I, z_W])$ and $B_r(z'_Q) \subset \mathcal{B}([z_I, z'_W])$, where

   $$\forall z_Q^* \in B_r(z_Q), \forall z_Q^\Delta \in B_r(z'_Q), f(z_I, z_W, z_Q^*) < f(z_I, z'_W, z_Q^\Delta). \tag{58}$$

   When we draw $z, z' \sim p(z)$, let C denote the event that this specific value of z_I is picked for both z, z', and we picked $z_{\setminus I} \in B_r(z'_Q)$, $z'_{\setminus I} \in B_r(z_Q)$. Since both balls have positive volume, $\Pr[C] > 0$. However, P does not happen whenever event C happens, since $z_I = z'_I$ but $f(z) > f(z')$, which contradicts $\Pr[P] = 1$.

2. Case 2: z_I is continuous.

   Similar to case 1, we can draw open balls of radius $r > 0$ around each point, i.e., $B_r(z_I, z_Q) \subset \mathcal{B}(z_W)$ and $B_r(z_I, z'_Q) \subset \mathcal{B}(z'_W)$, where

   $$\forall (z_I^*, z_Q^*) \in B_r(z_I, z_Q), \forall (z_I^\Delta, z_Q^\Delta) \in B_r(z_I, z'_Q), f(z_I^*, z_W, z_Q^*) < f(z_I^\Delta, z'_W, z_Q^\Delta). \tag{59}$$

Let $H^1 = \{(z_I^*, z_Q^*) \in B_r(z_I, z_Q) : z_I^* >= z_I\}$, $H^2 = \{(z_I^\Delta, z_Q^\Delta) \in B_r(z_I, z_Q') : z_I^\Delta <= z_I\}$. When we draw $z, z' \sim p(z)$, let C denote the event that we picked $z' \in H^1 \times \{z_W\}$, $z \in H^2 \times \{z_W'\}$. Since H^1, H^2 have positive volume, $\Pr[C] > 0$. However, P does not happen whenever event C happens, since $z_I <= z_I'$ but $f(z) > f(z')$, which contradicts $\Pr[P] = 1$.

Therefore we showed

$$\forall (z_I, z_W, z_Q), (z_I, z_W', z_Q') \in \mathcal{B}(Z), f(z_I, z_W, z_Q) = f(z_I, z_W', z_Q'), \tag{60}$$

i.e., g satisfies $C(I\,; p, g, e^*)$. By symmetry, e satisfies $C(I\,; p^*, g^*, e)$. □